

## Supporting Information

# Solid-Phase Synthesis of Oligodeoxynucleotides Using Nucleobase *N*-Unprotected the Oxazaphospholidine Derivatives a Bearing Long Alkyl Chain

*Kiyoshi Kakuta, Ryouta Kasahara, Kazuki Sato, Takeshi Wada\**

Department of Medicinal and Life Sciences, Faculty of Pharmaceutical Sciences, Tokyo University of  
Science, 2641 Yamazaki, Noda, Chiba 278-8510, Japan

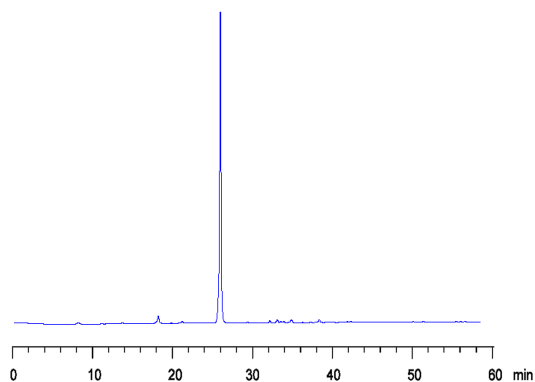
*E-mail: twada@rs.tus.ac.jp*

## Table of Contents

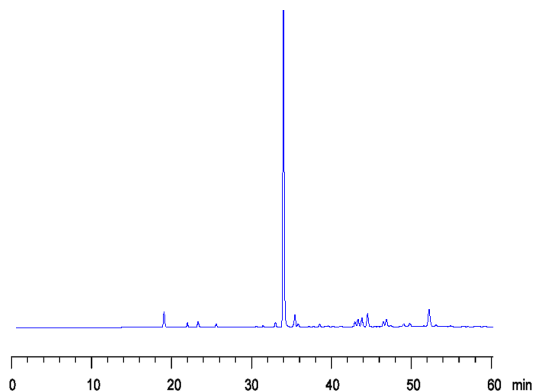
1. RP-HPLC profiles of dinucleotide phosphates (Table 1)	S3
2. RP-HPLC profiles of oligonucleotide phosphates (Table 1)	S5
3. Investigation of condensation efficiency after boronation (SI)	S6
4. RP-HPLC profiles of dinucleotide or trinucleotide boranophosphates (Table 2)	S8
5. RP-HPLC profiles of tetranucleotide bearing boranophosphate linkages (Table 3)	S10
6. RP-HPLC profiles of dodecamer bearing boranophosphate linkages (Scheme 4)	S11
7. $^1\text{H}$ , $^{13}\text{C}$ , $^{31}\text{P}$ NMR, COSY, HMQC, HMBC spectra	S12

**1. RP-HPLC profiles of dinucleotide phosphates (Table 1)**

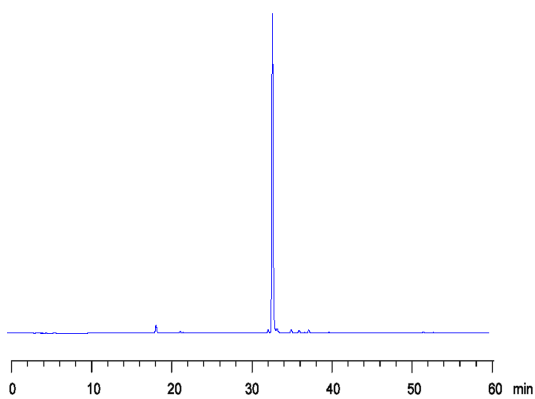
entry 1 (crude **10c** (**dC<sub>PO</sub>T**), **R = Me**)



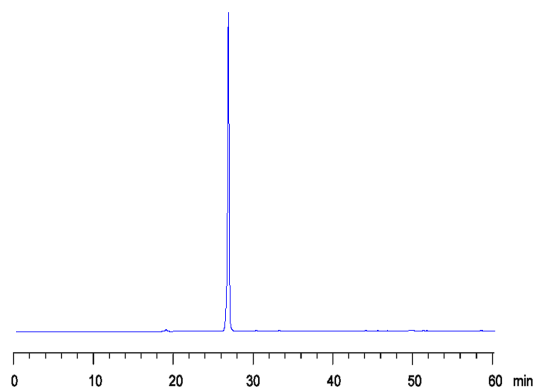
entry 2 (crude **10a** (**dA<sub>PO</sub>T**), **R = Me**)



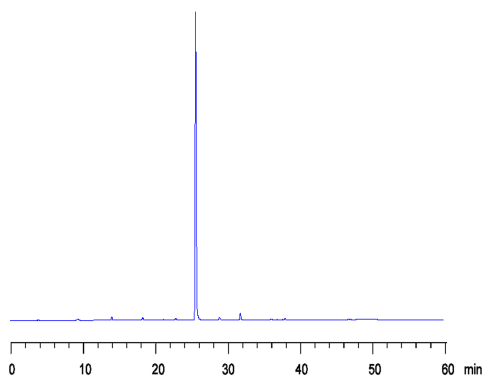
entry 3 (crude **10t** (**T<sub>PO</sub>T**), **R = Me**)



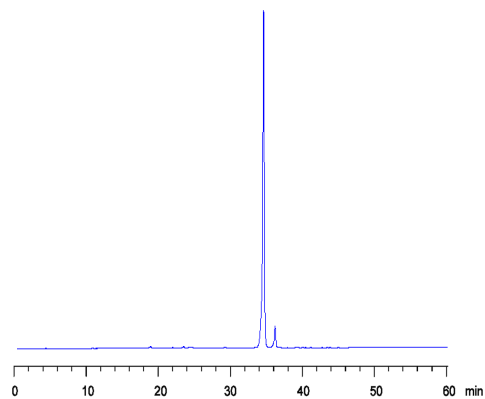
entry 4 (crude **10c** (**dC<sub>PO</sub>T**), **R = iPr**)



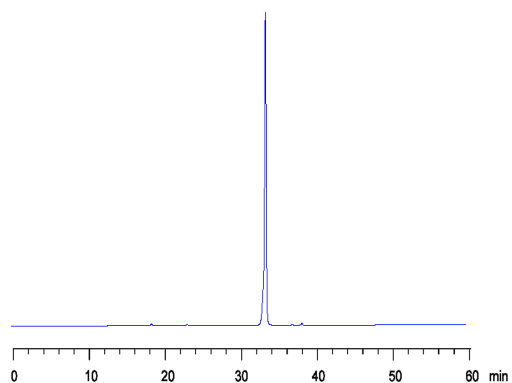
entry 5 (crude **10c** (**dC<sub>PO</sub>T**), **R = Thg**)



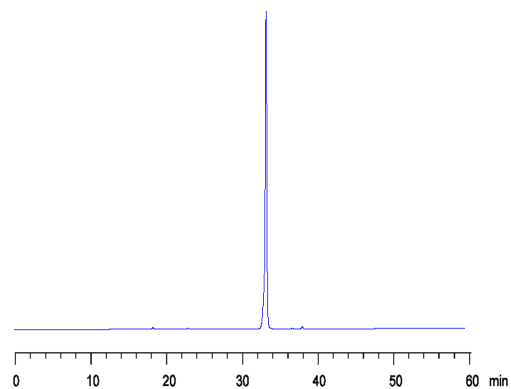
entry 6 (crude **10a** (**dA<sub>PO</sub>T**), **R = Thg**)



entry 7 (crude **10t** ( $T_{PO}T$ ), **R = Thg**)



entry 8 (crude **10g** ( $dG_{PO}T$ ), **R = Thg**)



entry 9 (crude **10l** ( $^L T_{PO}T$ ), **R = Thg**)

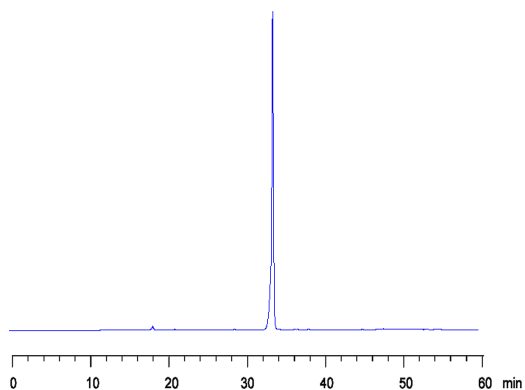
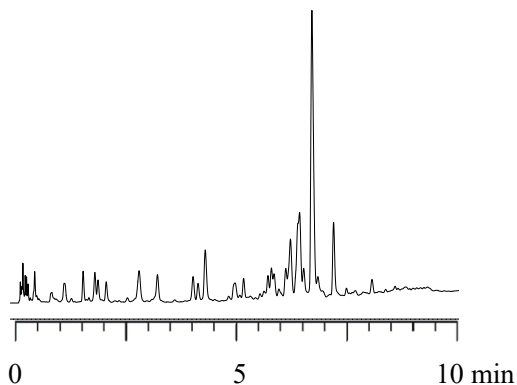


Figure S1 RP-HPLC profiles of the crude **10a-l** with detection at 260 nm. RP-HPLC was performed with a linear gradient of 0–20%  $CH_3CN$  for 60 min in 0.1 M TEAA buffer (pH 7.0) at 30 °C with a flow rate of 0.5 mL/min using a C18 column.

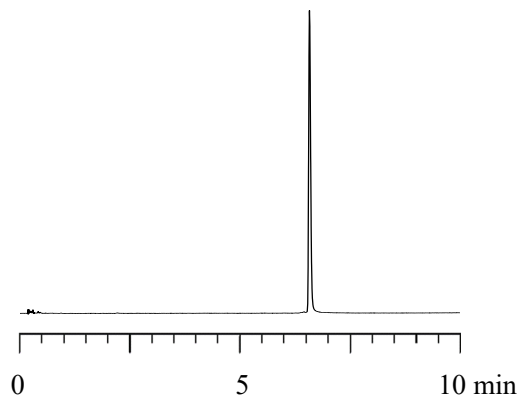
## 2. RP-HPLC profile of oligonucleotide phosphates (Table 1)

entry10 d(C<sub>P</sub>O A<sub>P</sub>O G<sub>P</sub>O T<sub>P</sub>O C<sub>P</sub>O A<sub>P</sub>O G<sub>P</sub>O T<sub>P</sub>O C<sub>P</sub>O A<sub>P</sub>O G<sub>P</sub>O T)

crude **11**



purified **11**



purchased **11**

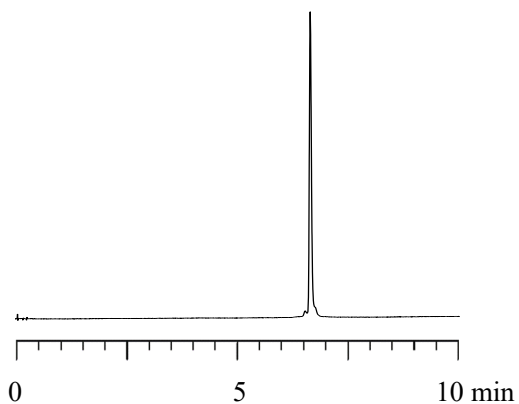


Figure S2 RP-HPLC profiles of the crude, the purified and the purchased **11** with detection at 260 nm. RP-UPLC was performed with a linear gradient of 5–25% MeOH for 10 min in a 0.4 M 1,1,1,3,3,3-hexafluoro-2-propanol, and 16 mM triethylamine at 50 °C with a flow rate of 0.5 mL/min using a C18 column. The product was eluted at 6.7 min.

### 3. Investigation of condensation efficiency after boronation (SI)

We investigated the condensation efficiency after a boronation because there is a possibility that the boronation reagent and/or its residue(s) inhibit the subsequent condensation reaction.

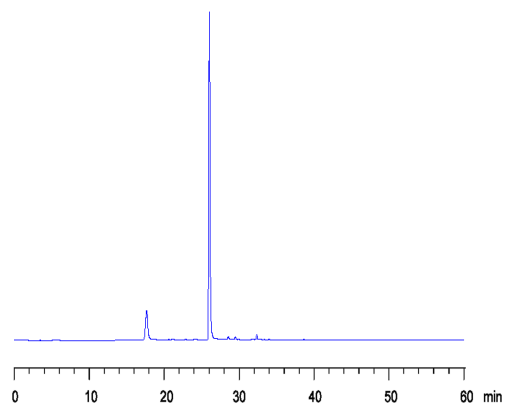
The HCP-loaded 5'-O-DMTr-Th (29.6  $\mu\text{mol/g}$ , 0.50  $\mu\text{mol}$ ), via a succinyl linker, was boronated using the boronation conditions of following Table S1. Afterward, the HCP was washed with dry THF ( $3 \times 1$  mL) and dry EtOH ( $3 \times 1$  mL) dry  $\text{CH}_2\text{Cl}_2$  ( $3 \times 1$  mL) and treated in a reaction vessel with 3% DCA in dry  $\text{CH}_2\text{Cl}_2$  ( $5 \times 12$  s, 1 mL each) and washed with dry  $\text{CH}_2\text{Cl}_2$  ( $3 \times 1$  mL) and  $\text{CH}_3\text{CN}$  ( $3 \times 1$  mL). Thereafter, it was dried in vacuo for 5 min. Then, the oxazaphospholidine monomer (**6c**, 30  $\mu\text{mol}$ ), which was dried in vacuo overnight, was added to the reaction vessel and dried in vacuo for 5 min. A 1.0 M solution of PhIMT (44.1 mg, 150  $\mu\text{mol}$ ) in dry  $\text{CH}_3\text{CN}$ -*i*PrCN (7:3, v/v, 150  $\mu\text{L}$ ), which was dried over MS 3 $\text{\AA}$  overnight, was added under Ar atmosphere to the reaction vessel. After 10 min, the HCP was washed with dry  $\text{CH}_3\text{CN}$  ( $3 \times 1$  mL) and dry  $\text{CH}_2\text{Cl}_2$  ( $3 \times 1$  mL) and dried in vacuo for 5 min. The resultant phosphite was oxidated upon treatment with a 1.0 M solution of TBHP (500  $\mu\text{L}$ , 500  $\mu\text{mol}$ ) in dry toluene and the reaction vessel was shaken for 5 min. Then, the HCP was washed with dry  $\text{CH}_2\text{Cl}_2$  ( $6 \times 1$  mL) and the detritylation reaction was carried out using 3% DCA in dry  $\text{CH}_2\text{Cl}_2$  ( $5 \times 12$  s, 1 mL each). Then, the HCP was washed with dry  $\text{CH}_2\text{Cl}_2$  ( $3 \times 1$  mL) and dry  $\text{CH}_3\text{CN}$  ( $3 \times 1$  mL). The HCP was then treated with a 25%  $\text{NH}_3$  aqueous solution–EtOH (3:1, v/v, 5 mL) at rt for 3 h, filtered, and washed with  $\text{CH}_3\text{CN}$ . The filtrate and the washings were combined, concentrated under reduced pressure, and the obtained residue was analyzed by RP-HPLC, which was performed with a linear gradient of 0–20%  $\text{CH}_3\text{CN}$  for 60 min in a 0.1 M TEAA buffer (pH 7.0).

**Table S1. Solid-Phase Synthesis of dC<sub>po</sub>T Dimers after botonated treatment in advance.**

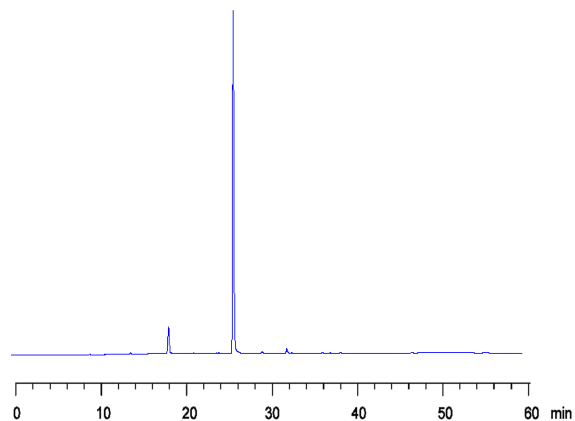
entry	boronation condition	T:10c <sup>a</sup>
1	1 M $\text{BH}_3 \cdot \text{SMe}_2$ /toluene for 15 min	14.4:85.6
2	1 M $\text{BH}_3 \cdot \text{THF}$ /THF for 15 min	6.7:93.3
3	0.05 M $\text{BH}_3 \cdot \text{THF}$ /THF for 15 min	2.5:97.5
4	0.05 M $\text{BH}_3 \cdot \text{THF}$ /THF for 2 min	1.6:98.4

<sup>a</sup> Determined by RP-HPLC.

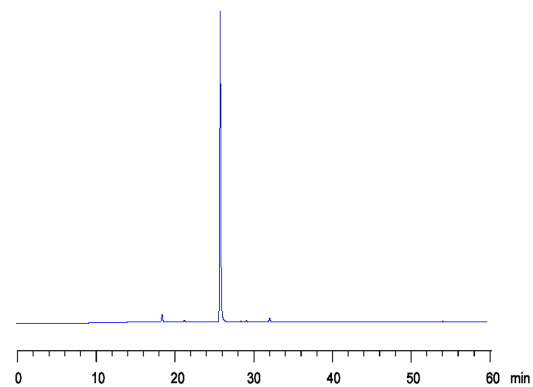
entry 1



entry 2



entry 3



entry 4

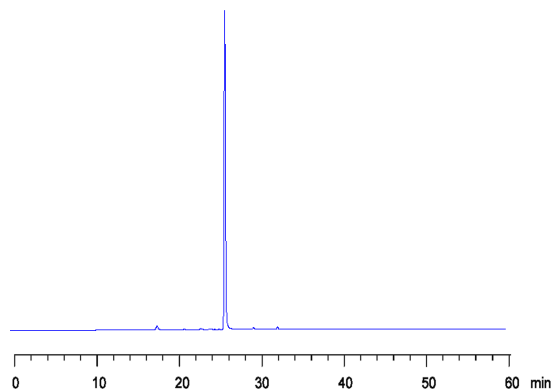
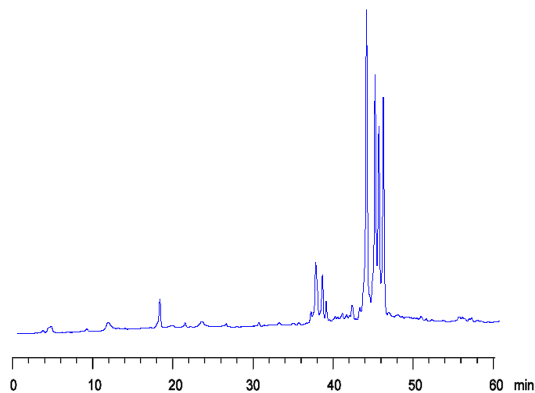
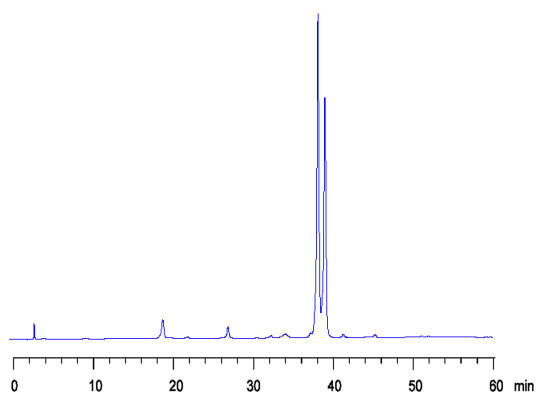


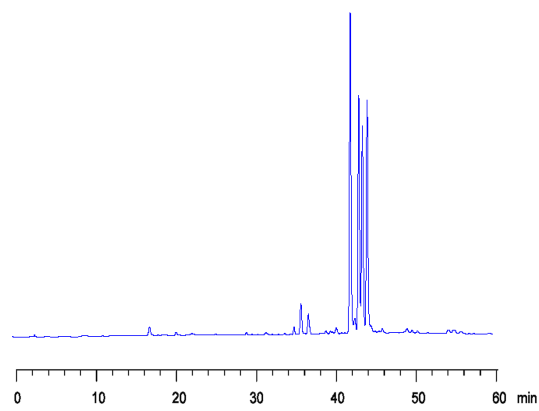
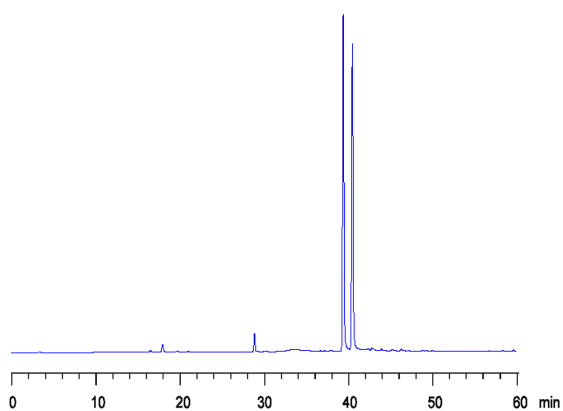
Figure S3 RP-HPLC profiles of crude **10c** with detection at 260 nm. RP-HPLC was performed with a linear gradient of 0–20% CH<sub>3</sub>CN for 60 min in 0.1 M TEAA buffer (pH 7.0) at 30 °C with a flow rate of 0.5 mL/min using a C18 column.

**4. RP-HPLC profiles of dinucleotide or trinucleotide boranophosphates (Table2)**  
entry 1 (crude **14c** (**dC<sub>PB</sub>T**)) entry 2 (crude **15** (**d(C<sub>PB</sub>C<sub>PB</sub>T**)))



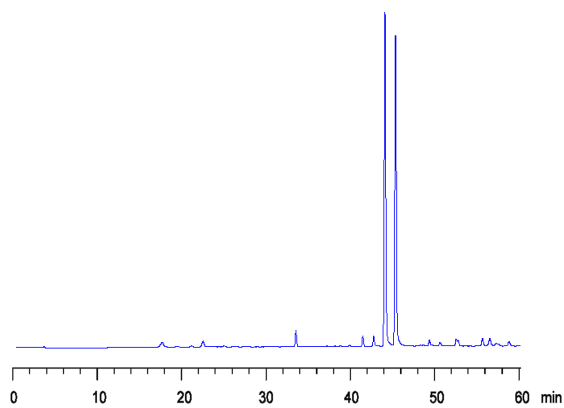
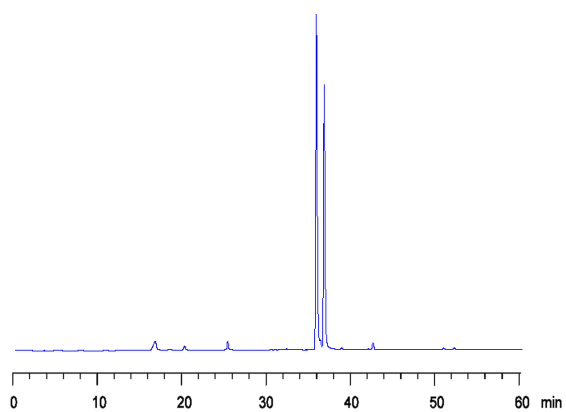
entry 3 (crude **14c** (**dC<sub>PB</sub>T**))

entry 4 (crude **15** (**d(C<sub>PB</sub>C<sub>PB</sub>T**)))



entry 5 (crude **14c** (**dA<sub>PB</sub>T**))

entry 6 (crude **14g** (**dG<sub>PB</sub>T**))





entry 7 (crude **14t** (**T<sub>PB</sub>T**))

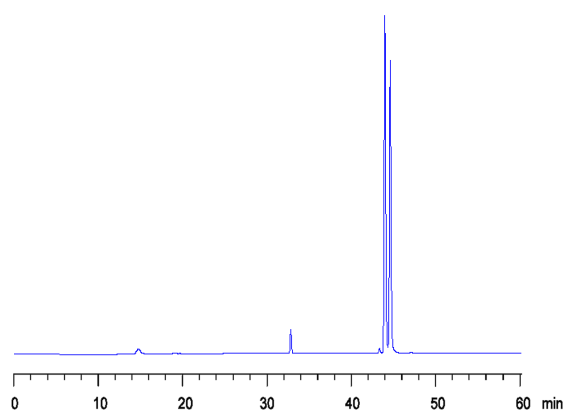
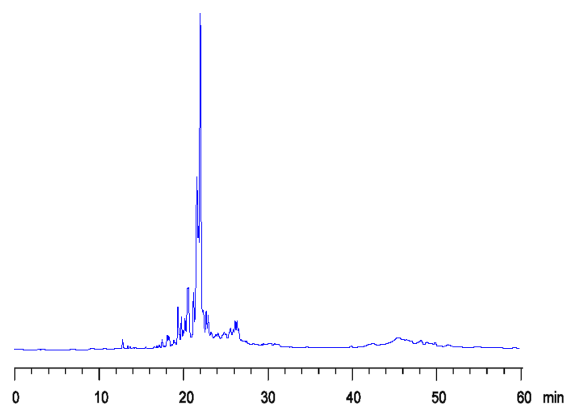


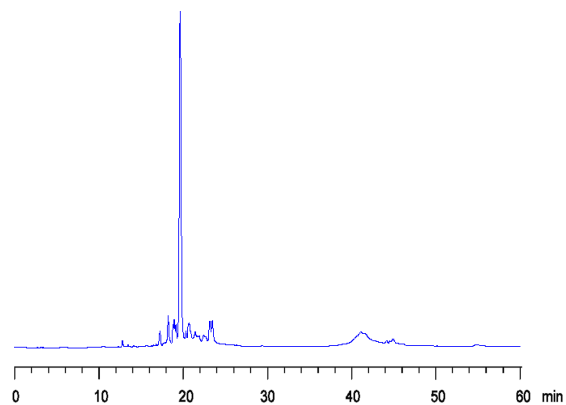
Figure S4 RP-HPLC profiles of crude **14a-t** and **15** with detection at 260 nm. RP-HPLC was performed with a linear gradient of 0–20% CH<sub>3</sub>CN for 60 in 0.1 M TEAA buffer (pH 7.0) at 30 °C min with a flow rate of 0.5 mL/min using a C18 column.

## 5. RP-HPLC profiles of tetranucleotide bearing boranophosphate linkages (Table3)

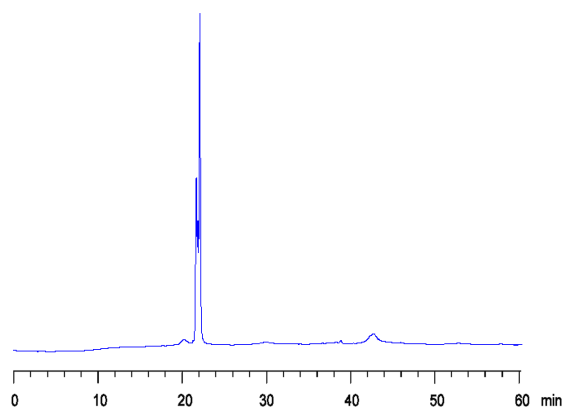
entry 1 (crude **16** ( $d(C_{PB}A_{PB}G_{PB}T)$ ))



entry 2 (crude **17** ( $d(C_{PB}A_{PO}G_{PB}T)$ ))



purified **16**



purified **17**

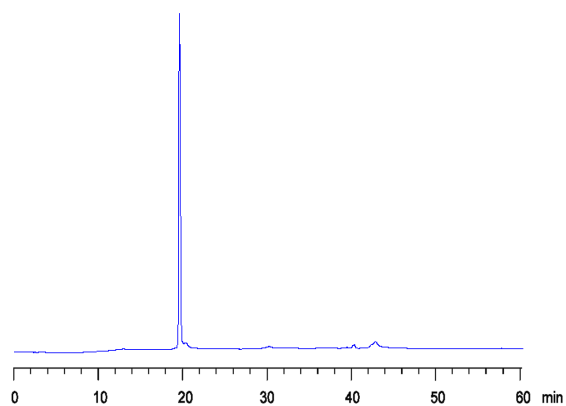


Figure S5 RP-HPLC profiles of the crude **16, 17** and purified **16, 17** with detection at 260 nm. RP-HPLC was performed with a linear gradient of 0–60%  $CH_3CN$  for 60 min in 0.1 M TEAA buffer (pH 7.0) at 30 °C with a flow rate of 0.5 mL/min using a C18 column.

**6. RP-HPLC profiles of dodecamer bearing boranophosphate linkages (Scheme 4)**  
**d(C<sub>PBA</sub>POG<sub>PB</sub>C<sub>PO</sub>T<sub>PBA</sub>POG<sub>PB</sub>T<sub>PO</sub>C<sub>PBA</sub>POG<sub>PB</sub>T)**

crude **18**

purified **18**

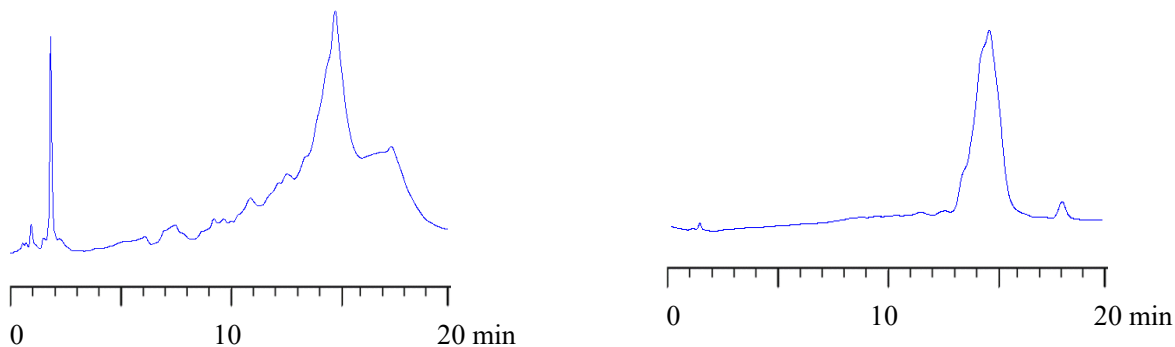
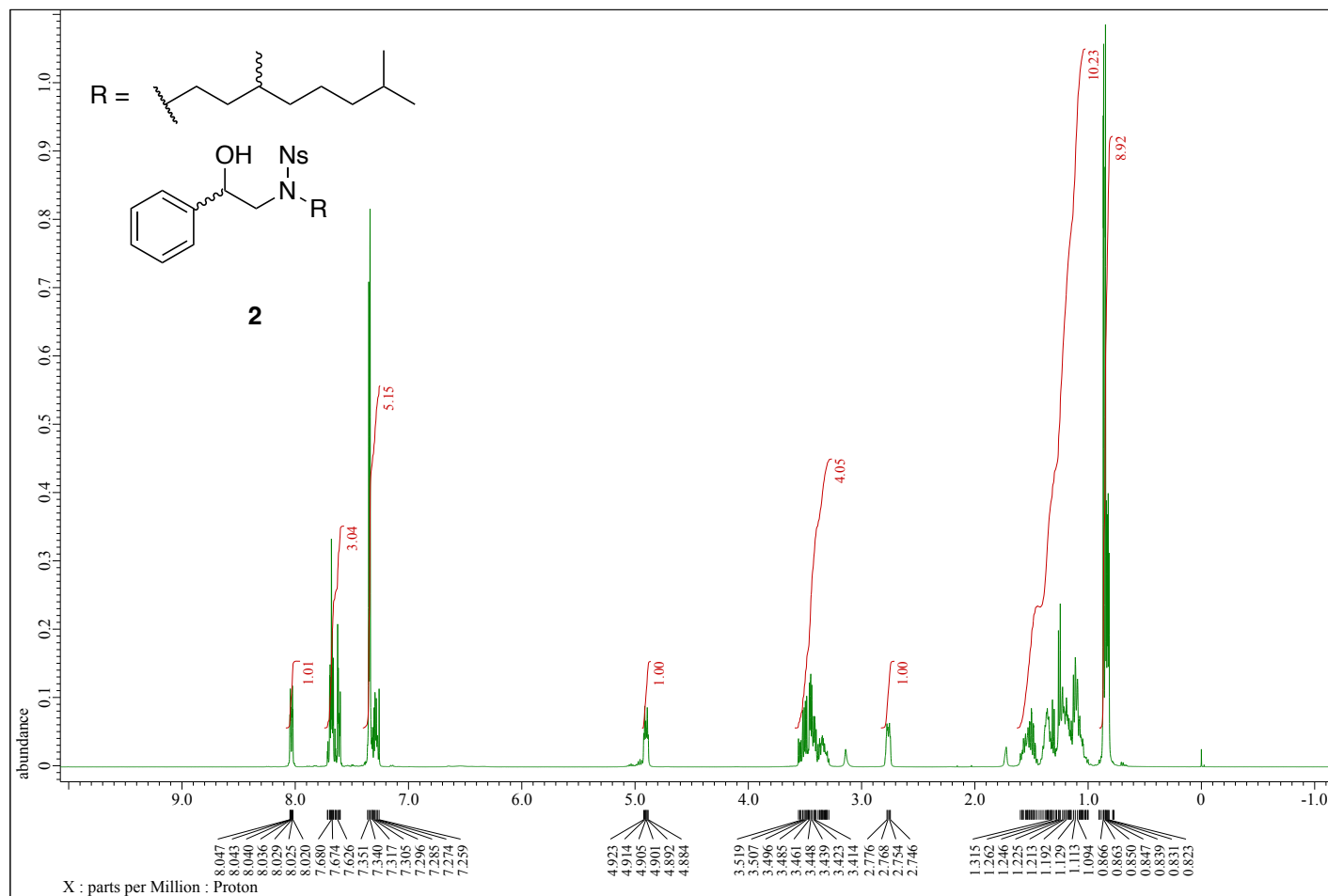


Figure S6 RP-HPLC profiles of crude **18** and purified **18** with detection at 260 nm. RP-HPLC was performed with a linear gradient of 5–40% MeOH for 20 min in 0.4 M 1,1,1,3,3,3-hexafluoro-2-propanol and 8 mM triethylamine at 60 °C with a flow rate of 0.5 mL/min using a C18 column.

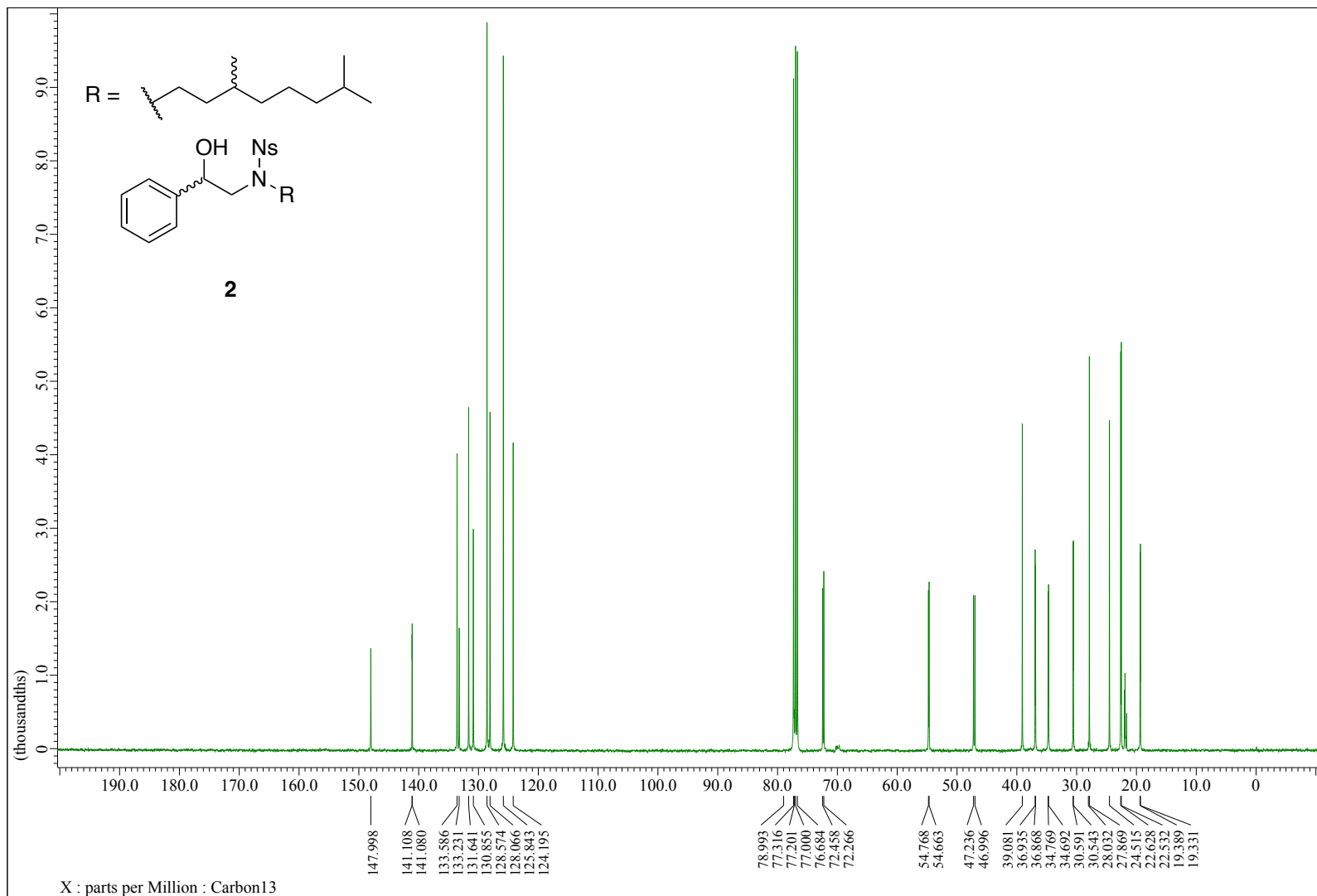
## 7. $^1\text{H}$ , $^{13}\text{C}$ , $^{31}\text{P}$ , COSY, HMQC, HMBC NMR spectra

*N*-(3,7-Dimethyloctyl)-*N*-(2-hydroxy-2-phenylethyl)-2-nitrobenzenesulfonamide (**2**)

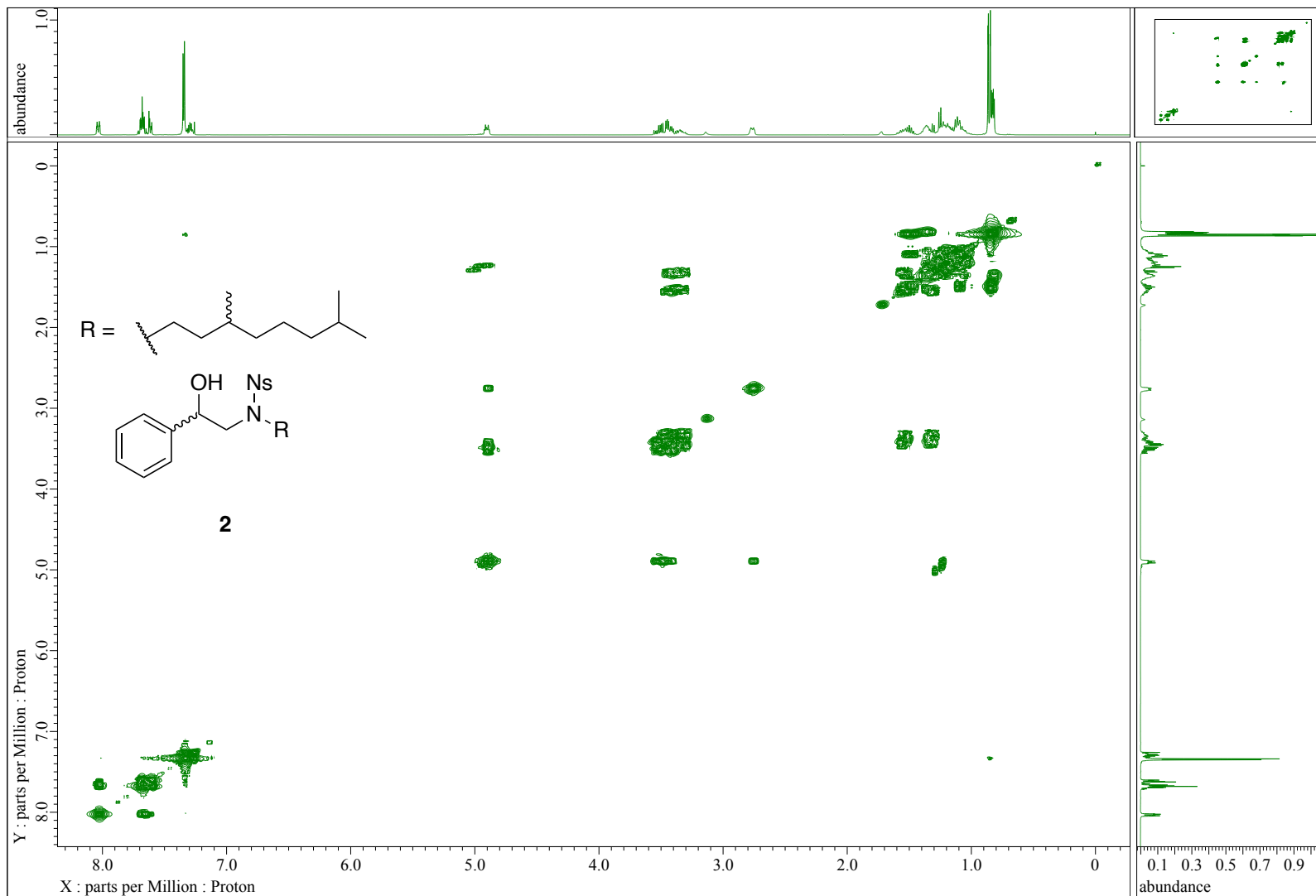
$^1\text{H}$  NMR (400 MHz,  $\text{CDCl}_3$ )



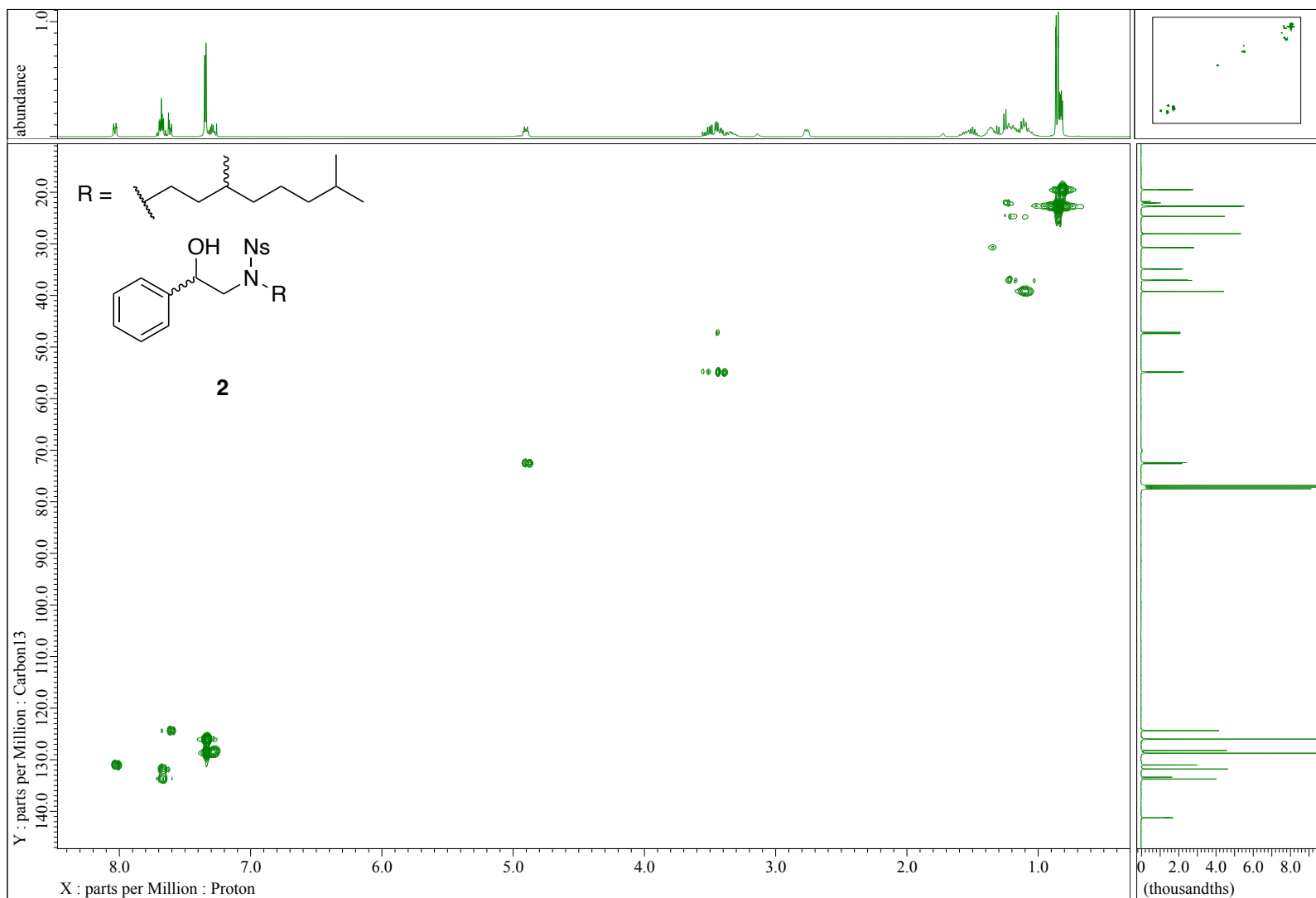
$^{13}\text{C}$   $\{^1\text{H}\}$  NMR (101 MHz,  $\text{CDCl}_3$ )



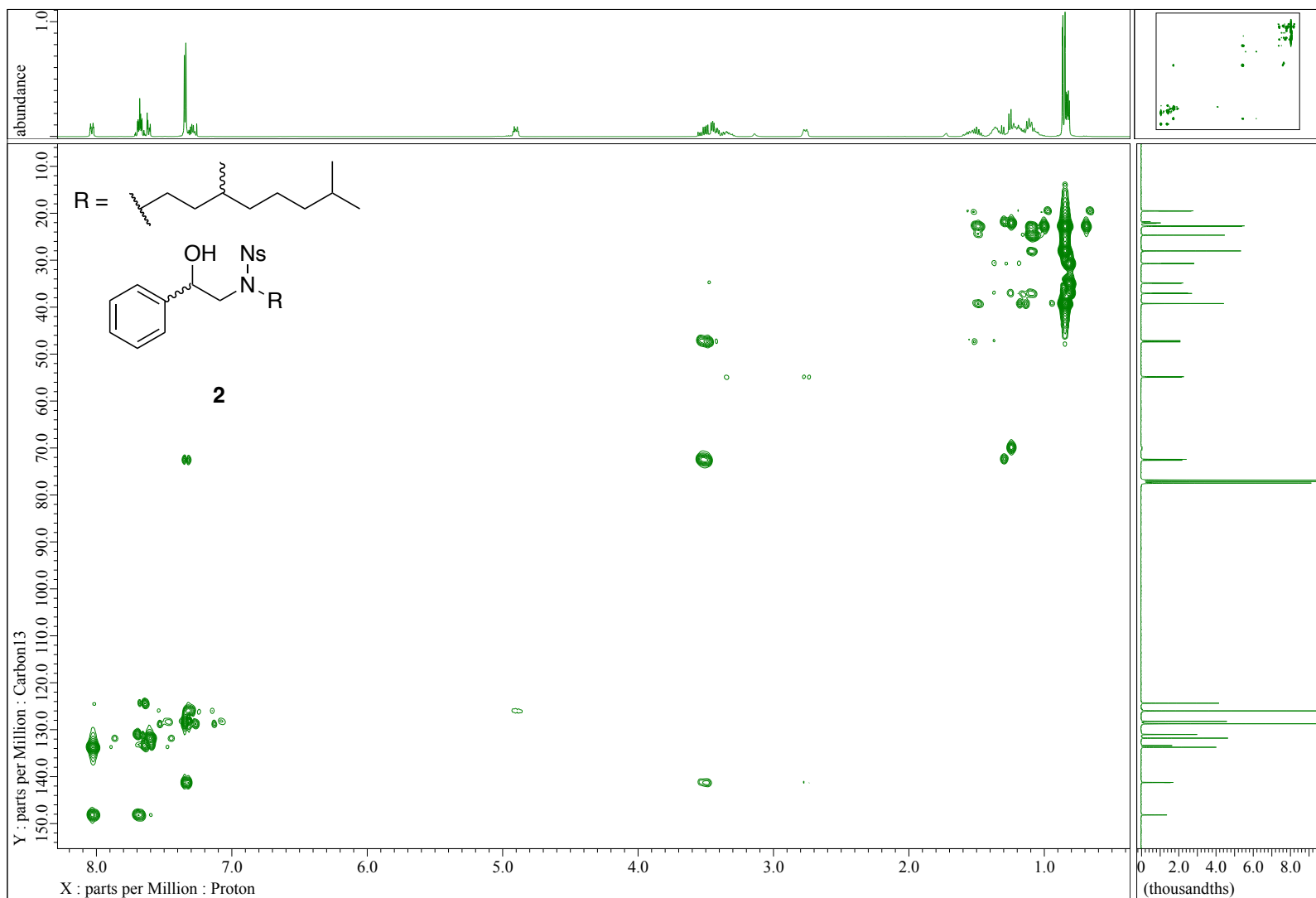
COSY (CDCl<sub>3</sub>)



# HMQC (CDCl<sub>3</sub>)

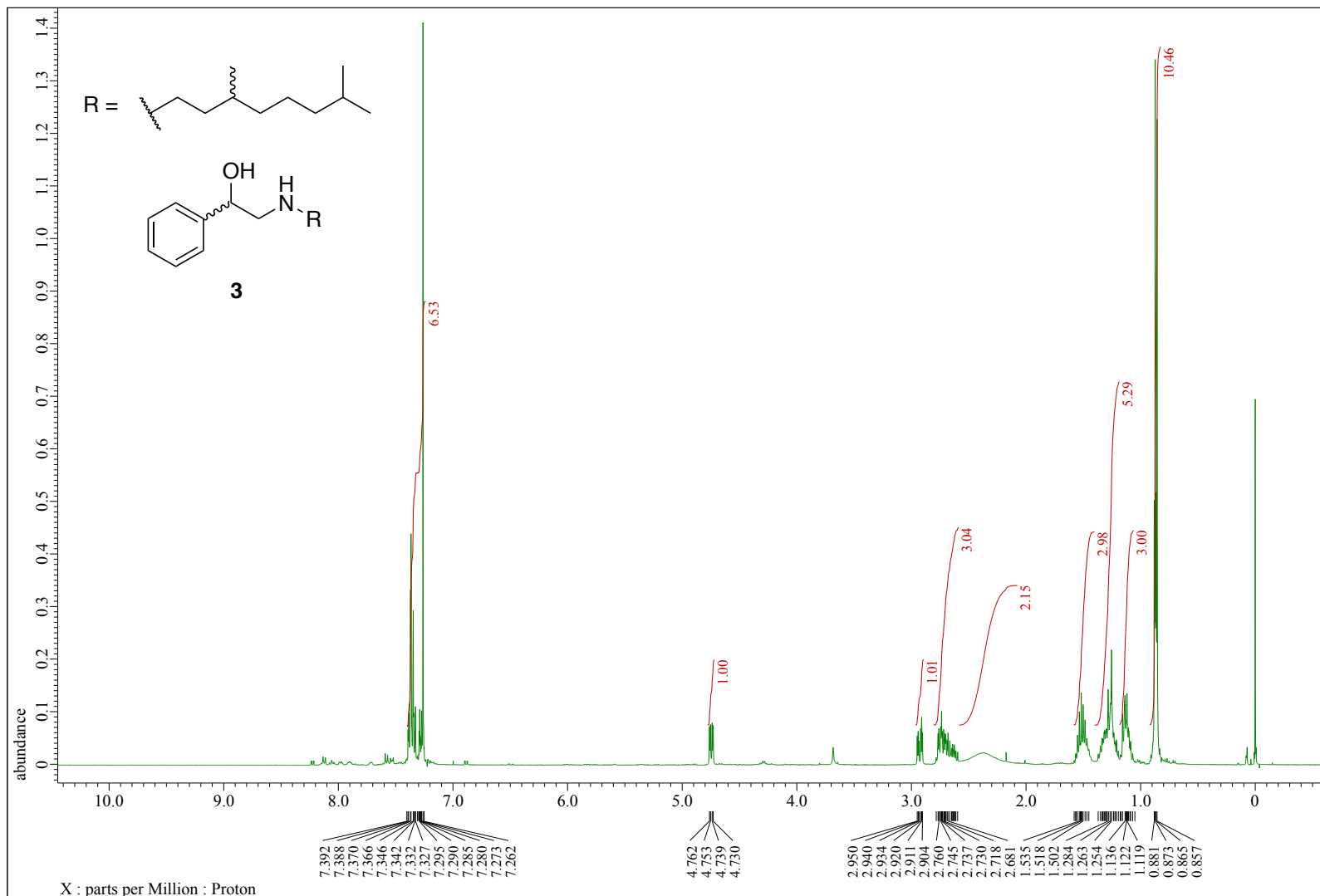


# HMBC (CDCl<sub>3</sub>)

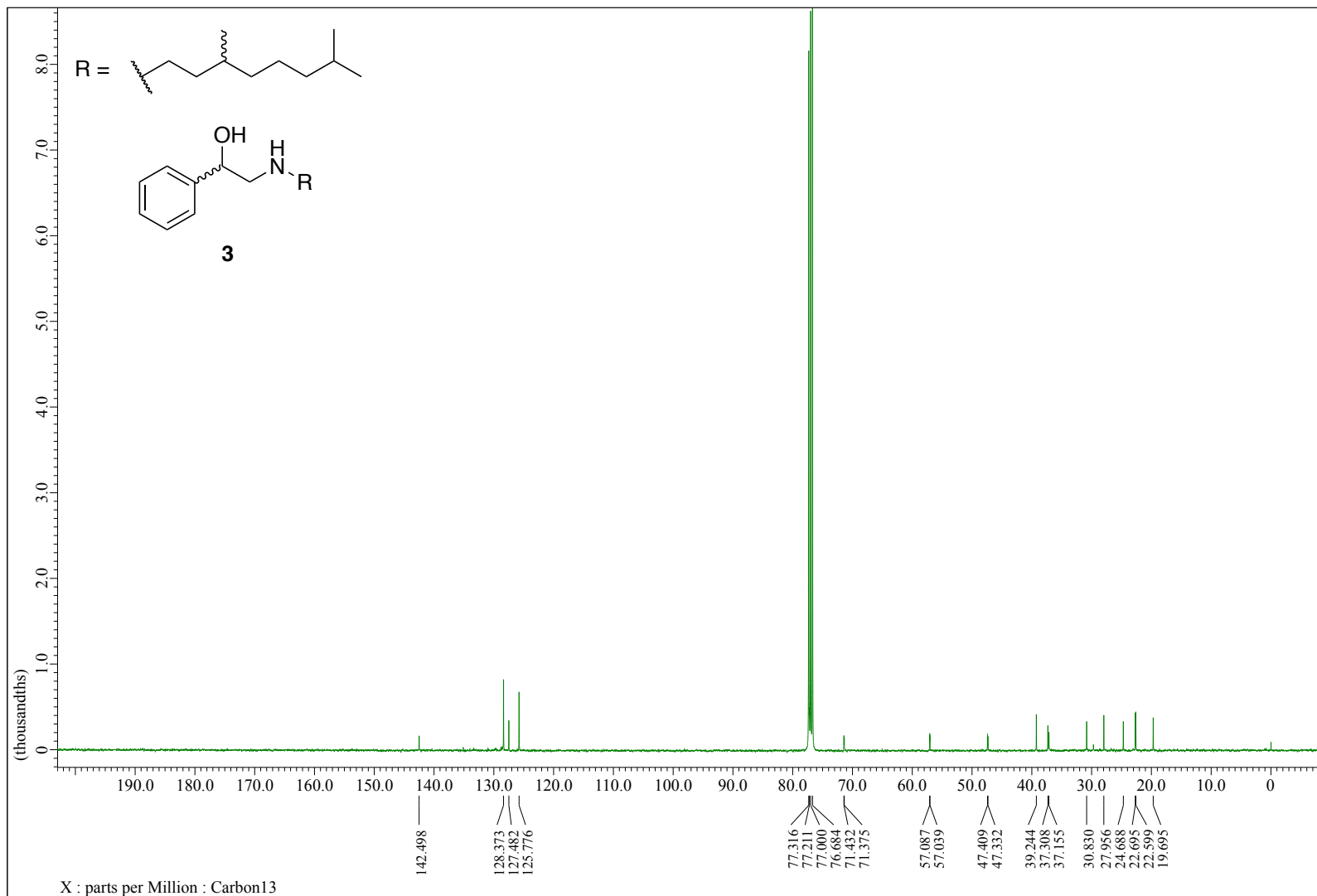




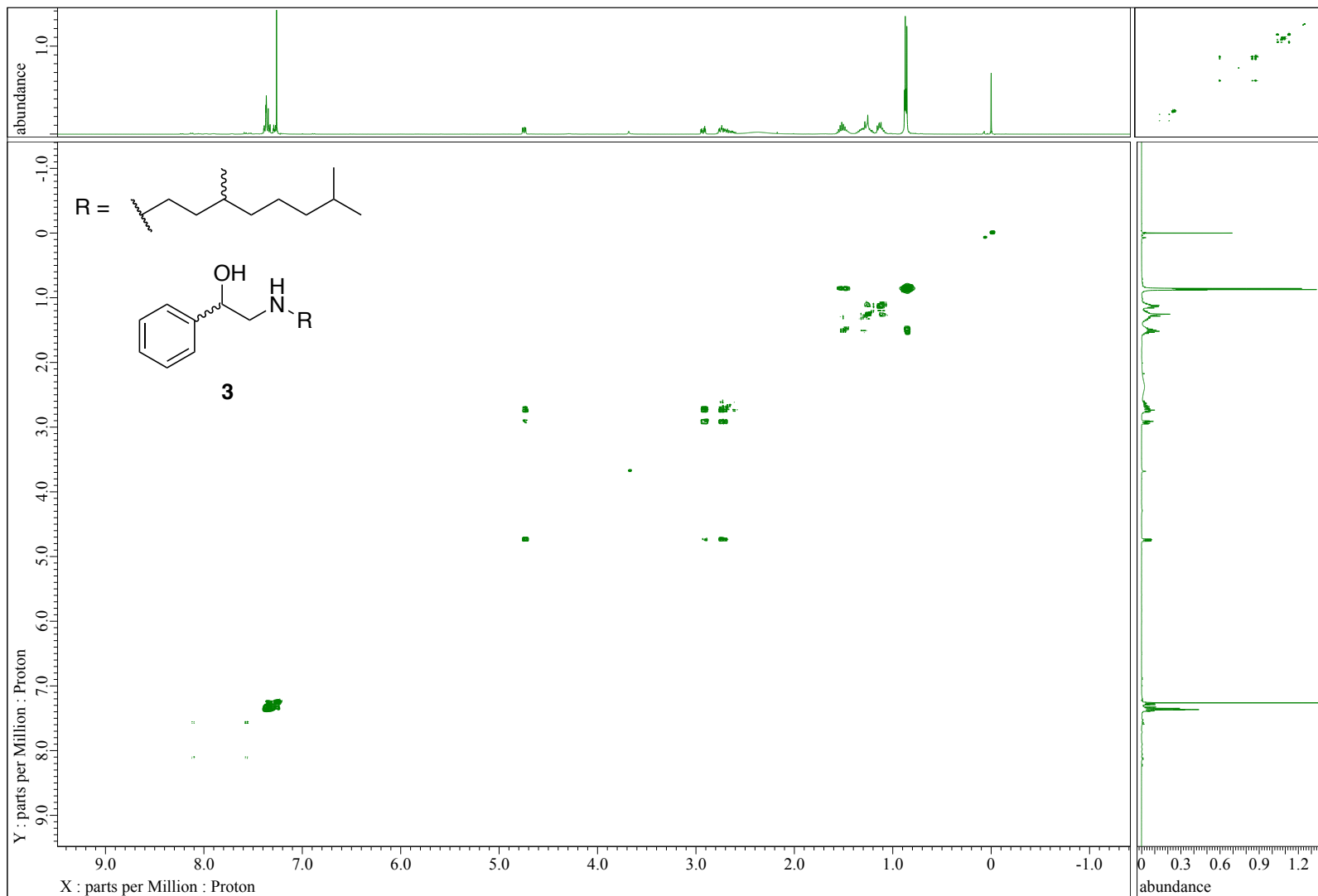
2-((3,7-Dimethyloctyl)amino)-1-phenylethan-1-ol (3)  
<sup>1</sup>H NMR (400 MHz, CDCl<sub>3</sub>)



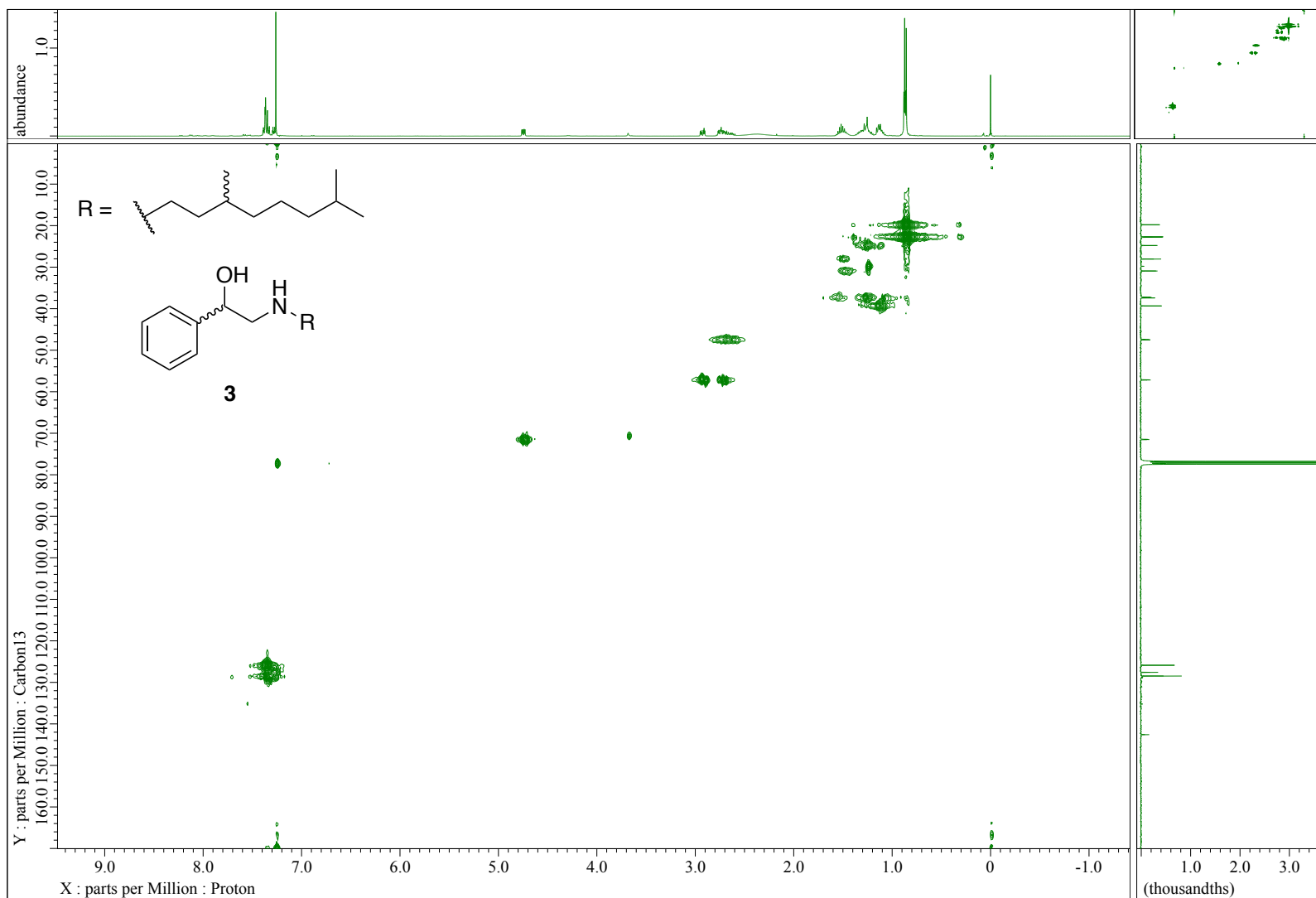
$^{13}\text{C}$   $\{^1\text{H}\}$  NMR (101 MHz,  $\text{CDCl}_3$ )



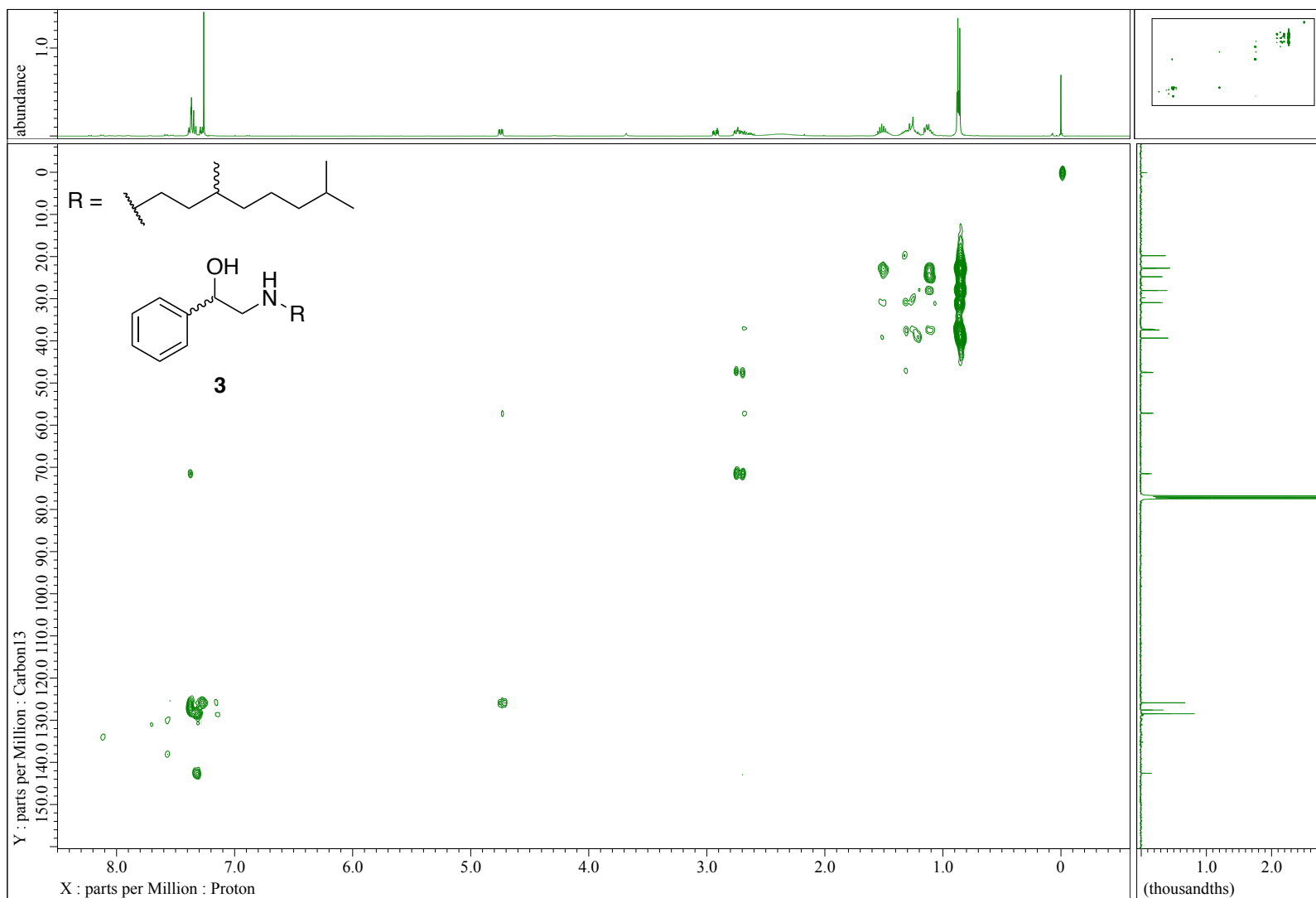
# COSY (CDCl<sub>3</sub>)



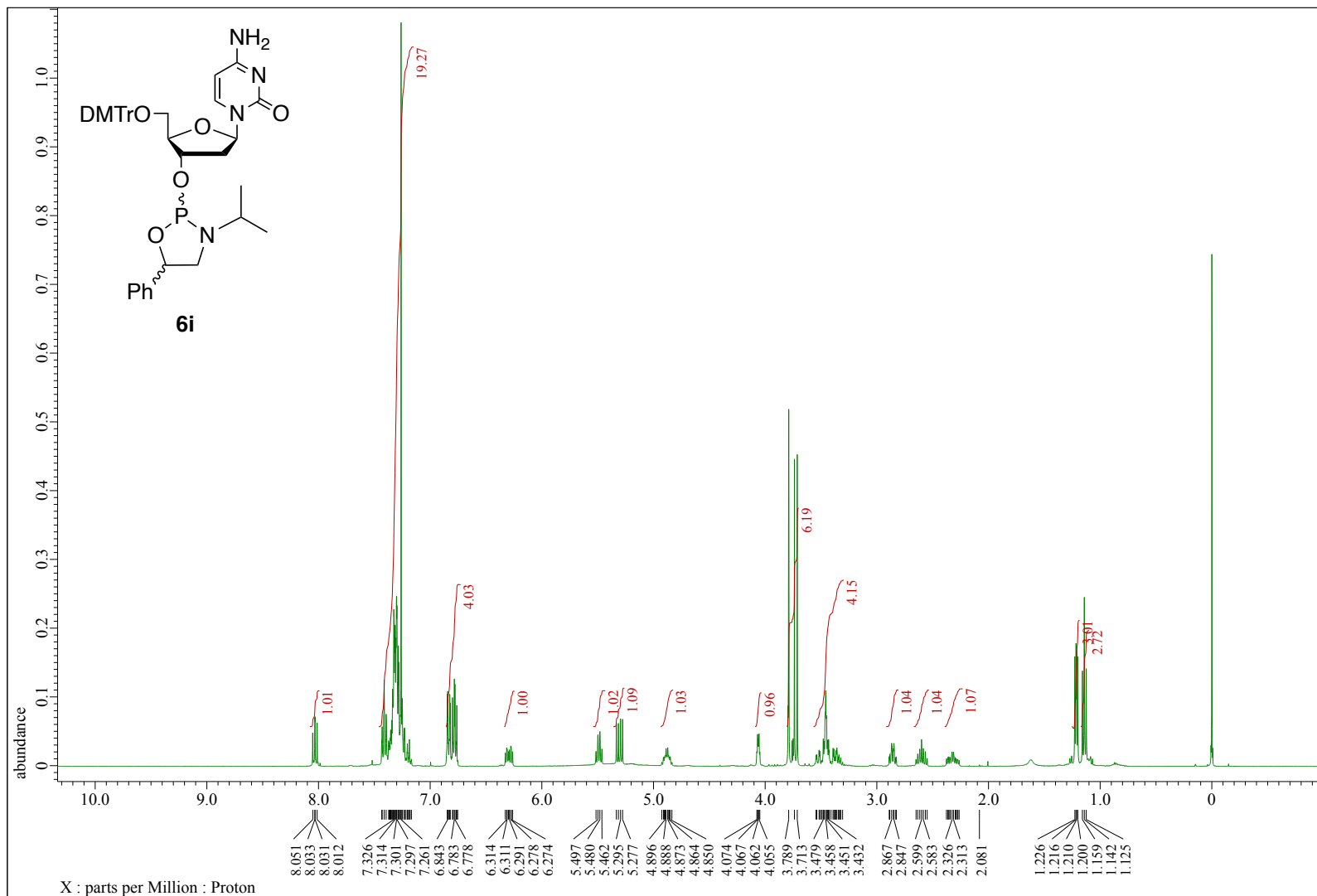
# HMQC (CDCl<sub>3</sub>)



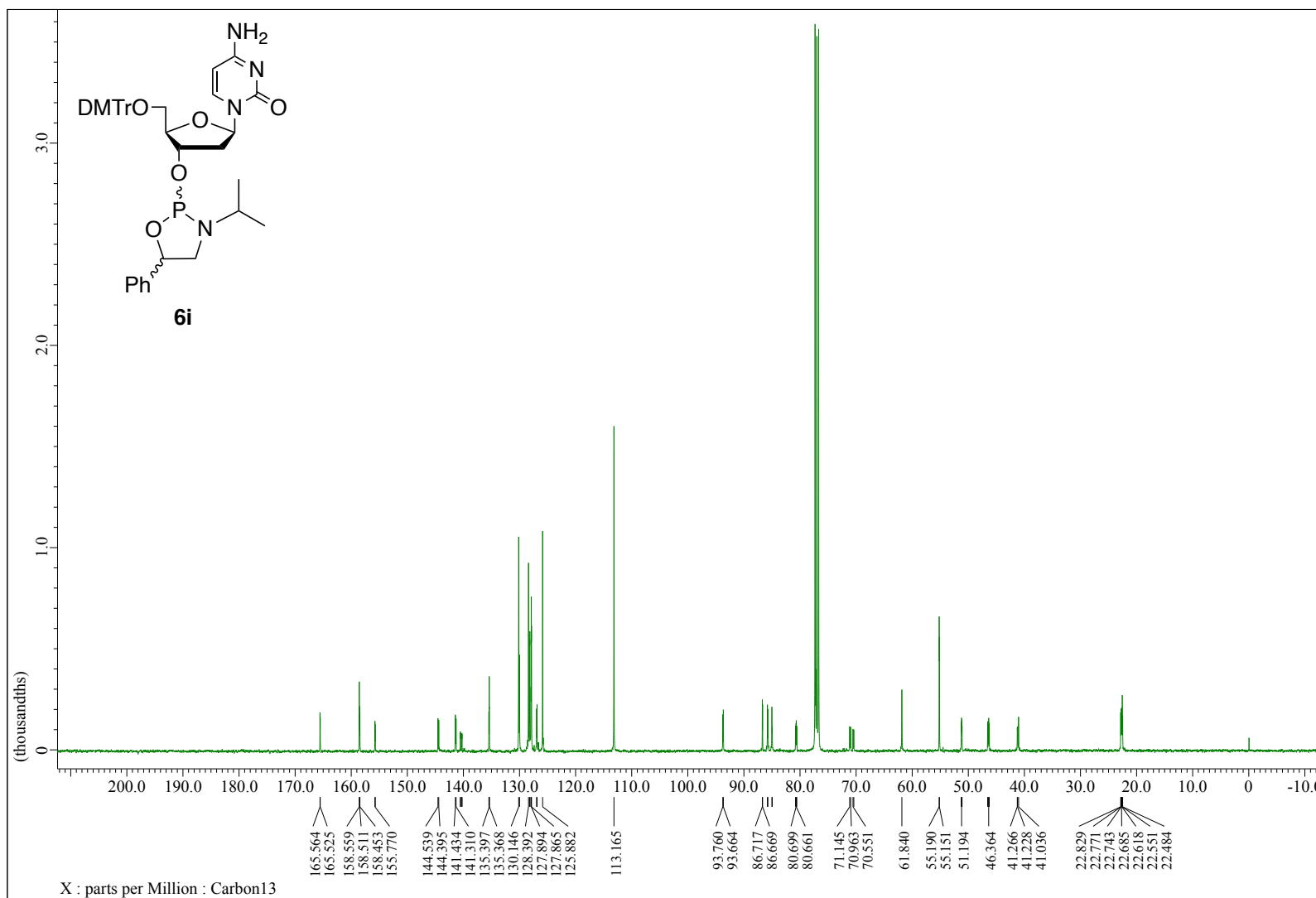
# HMBC (CDCl<sub>3</sub>)



**dCy oxazaphospholidine *N*-*i*Pr monomer (6i)**  
**<sup>1</sup>H NMR (400 MHz, CDCl<sub>3</sub>)**

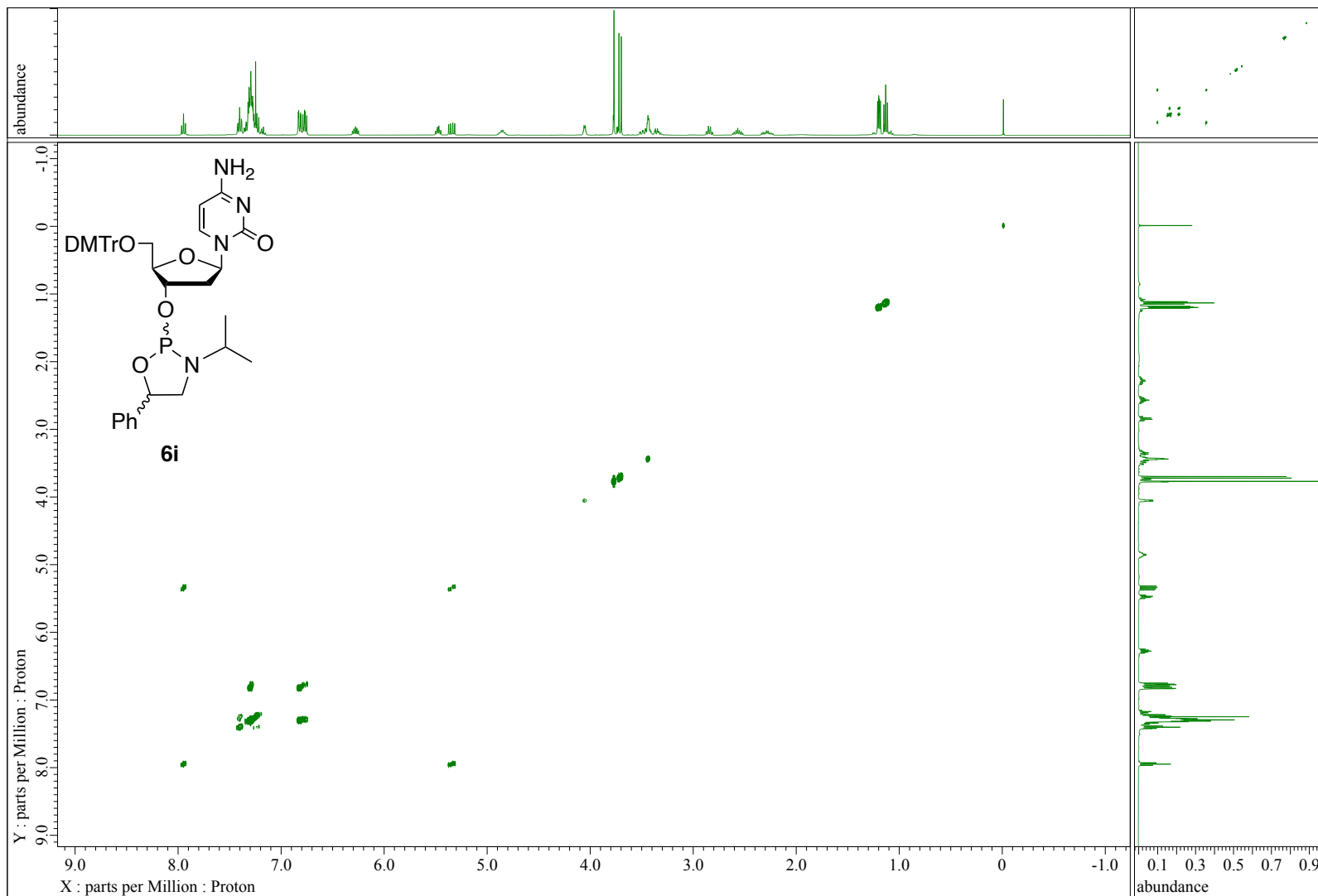


$^{13}\text{C}$   $\{^1\text{H}\}$  NMR (101 MHz,  $\text{CDCl}_3$ )



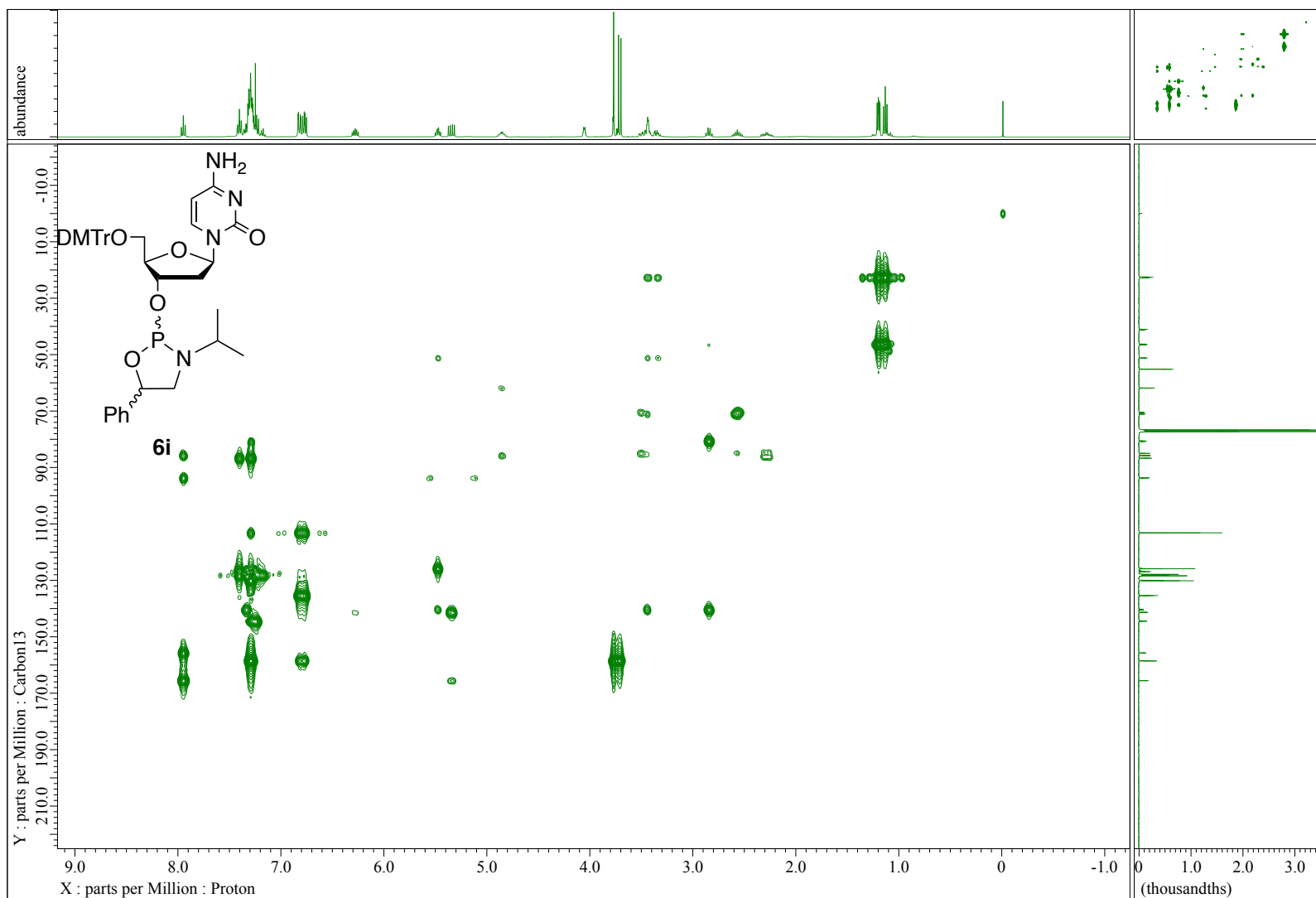
$^{31}\text{P}$   $\{^1\text{H}\}$  NMR (162 MHz,  $\text{CDCl}_3$ )

COSY (CDCl<sub>3</sub>)

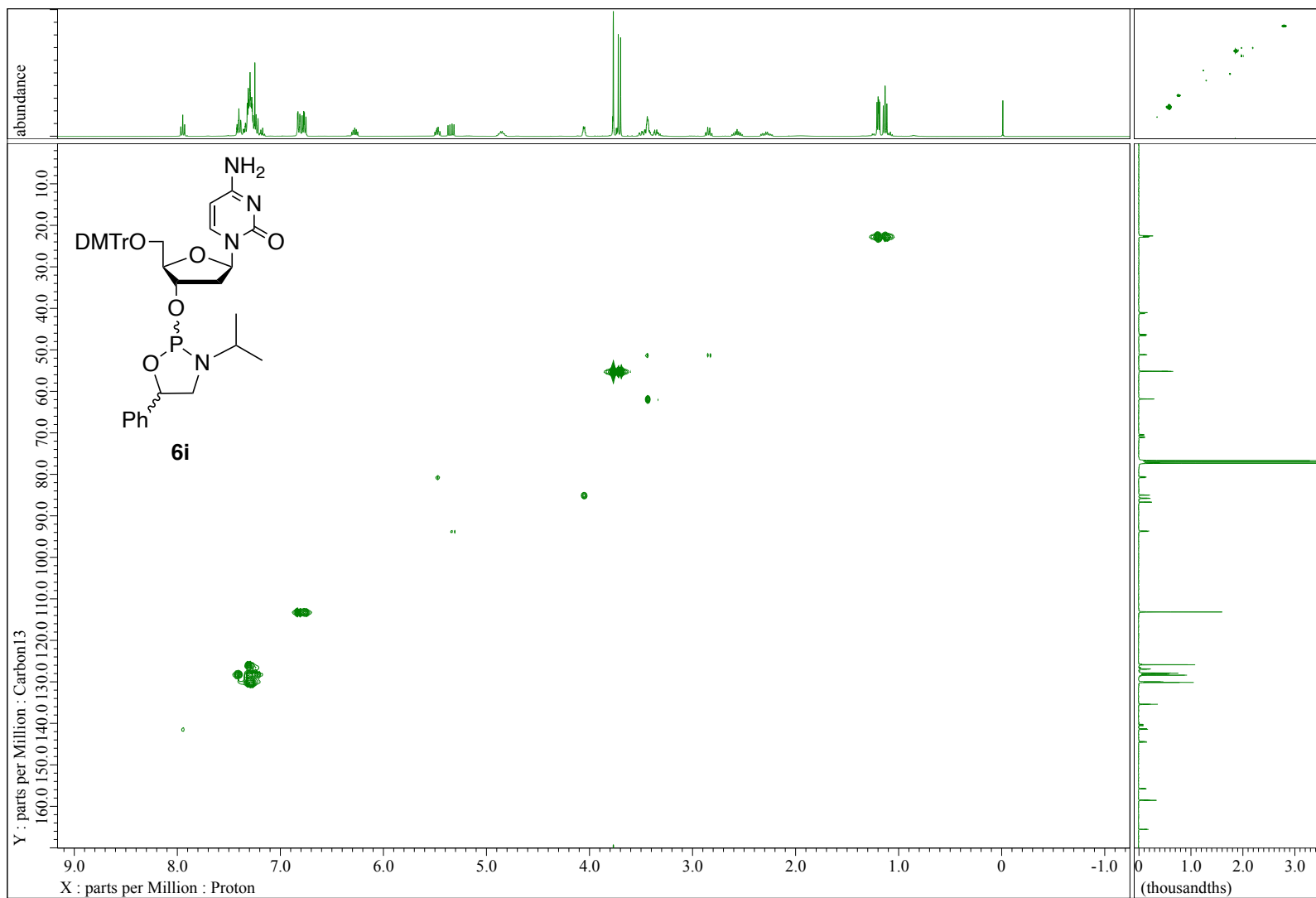




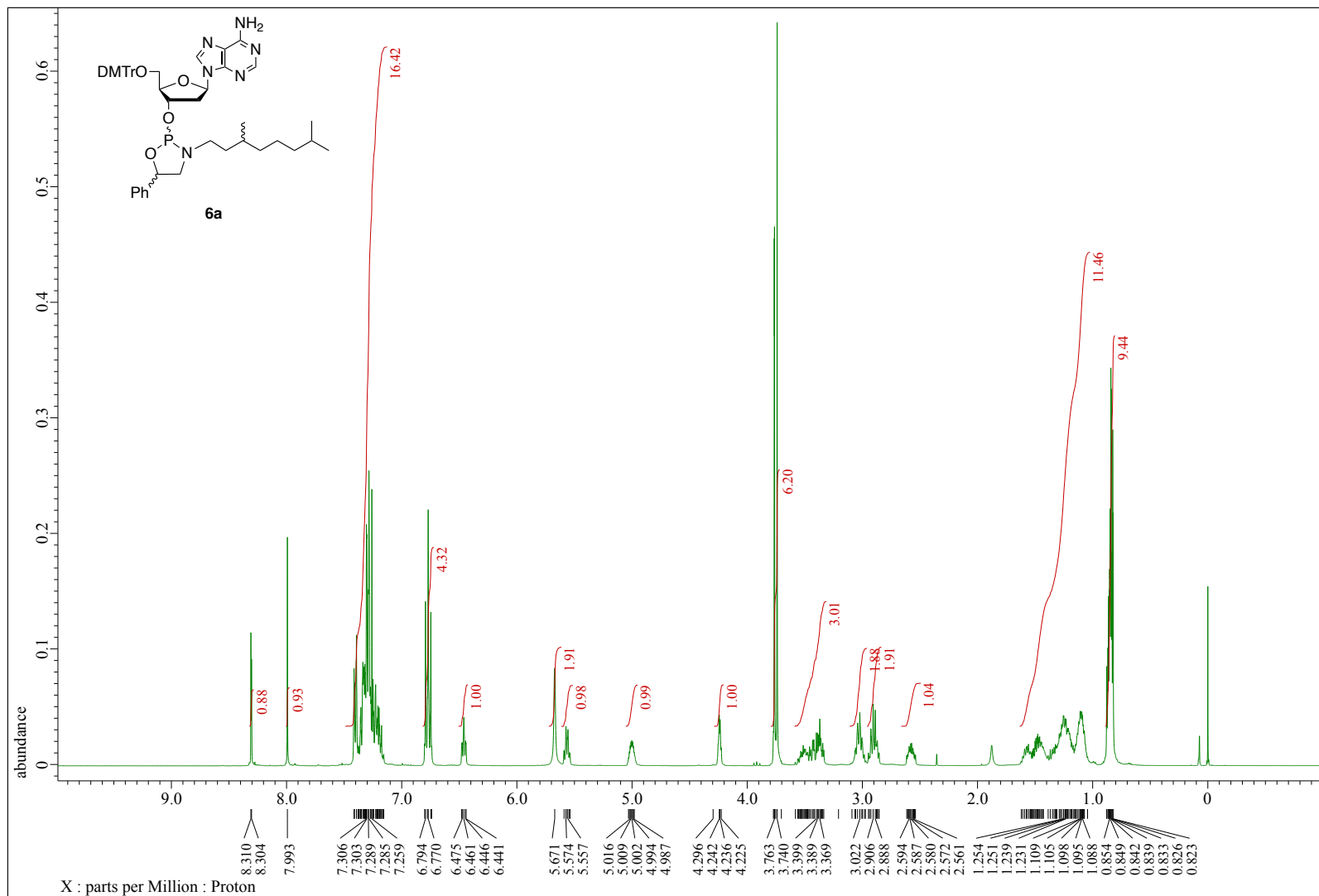
# HMQC (CDCl<sub>3</sub>)



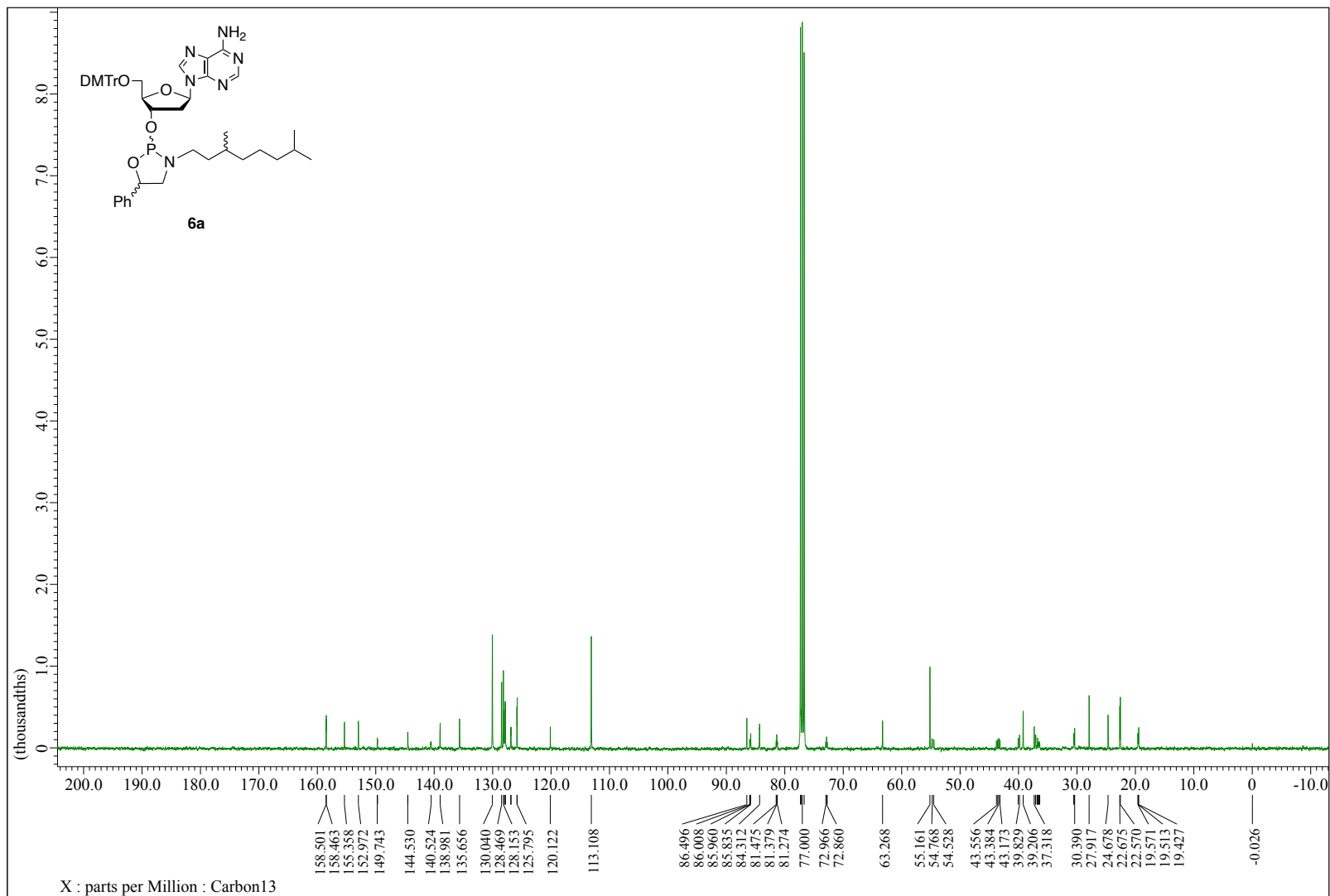
# HMBC (CDCl<sub>3</sub>)



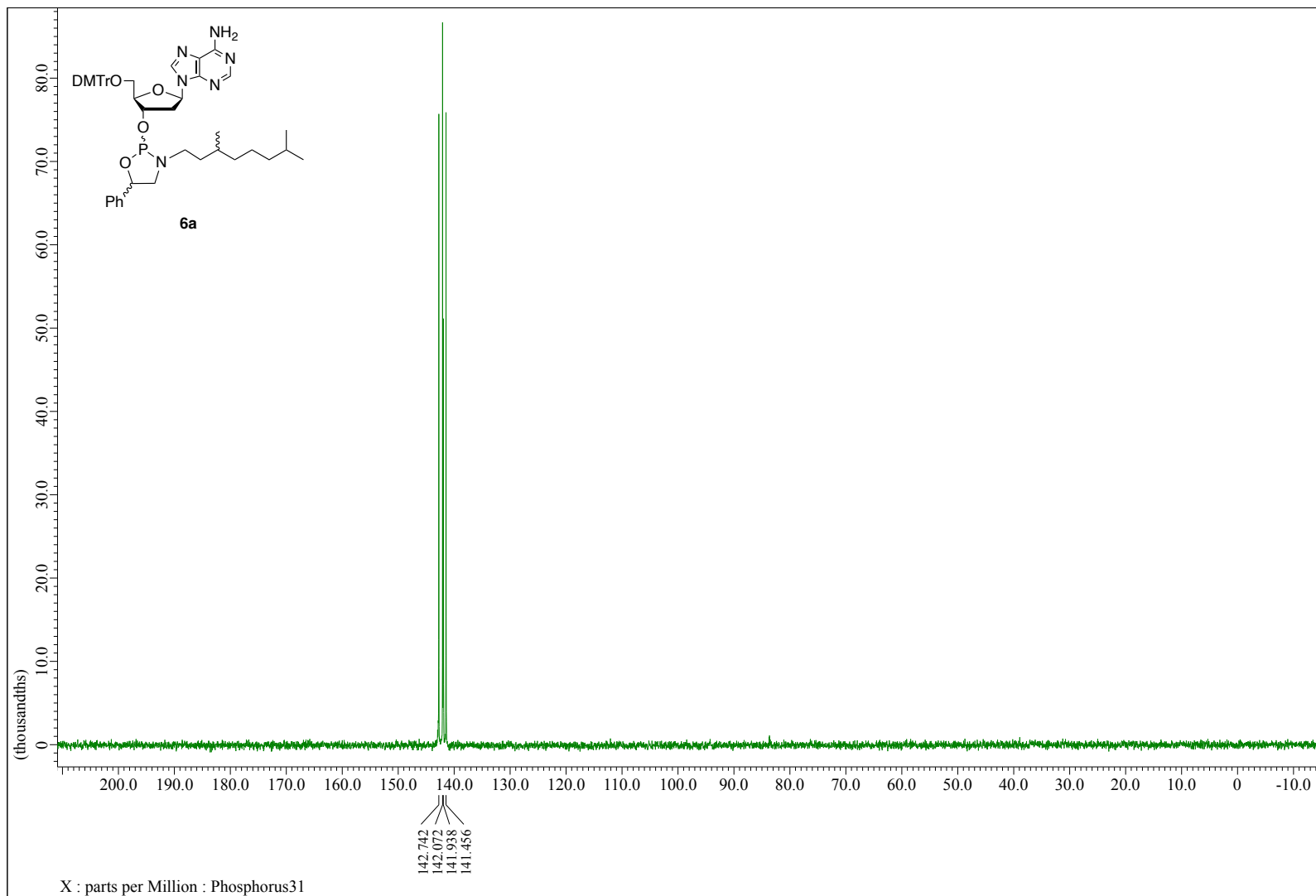
**dAd oxazaphospholidine *N*-Thg monomer (6a)**  
**<sup>1</sup>H NMR (400 MHz, CDCl<sub>3</sub>)**



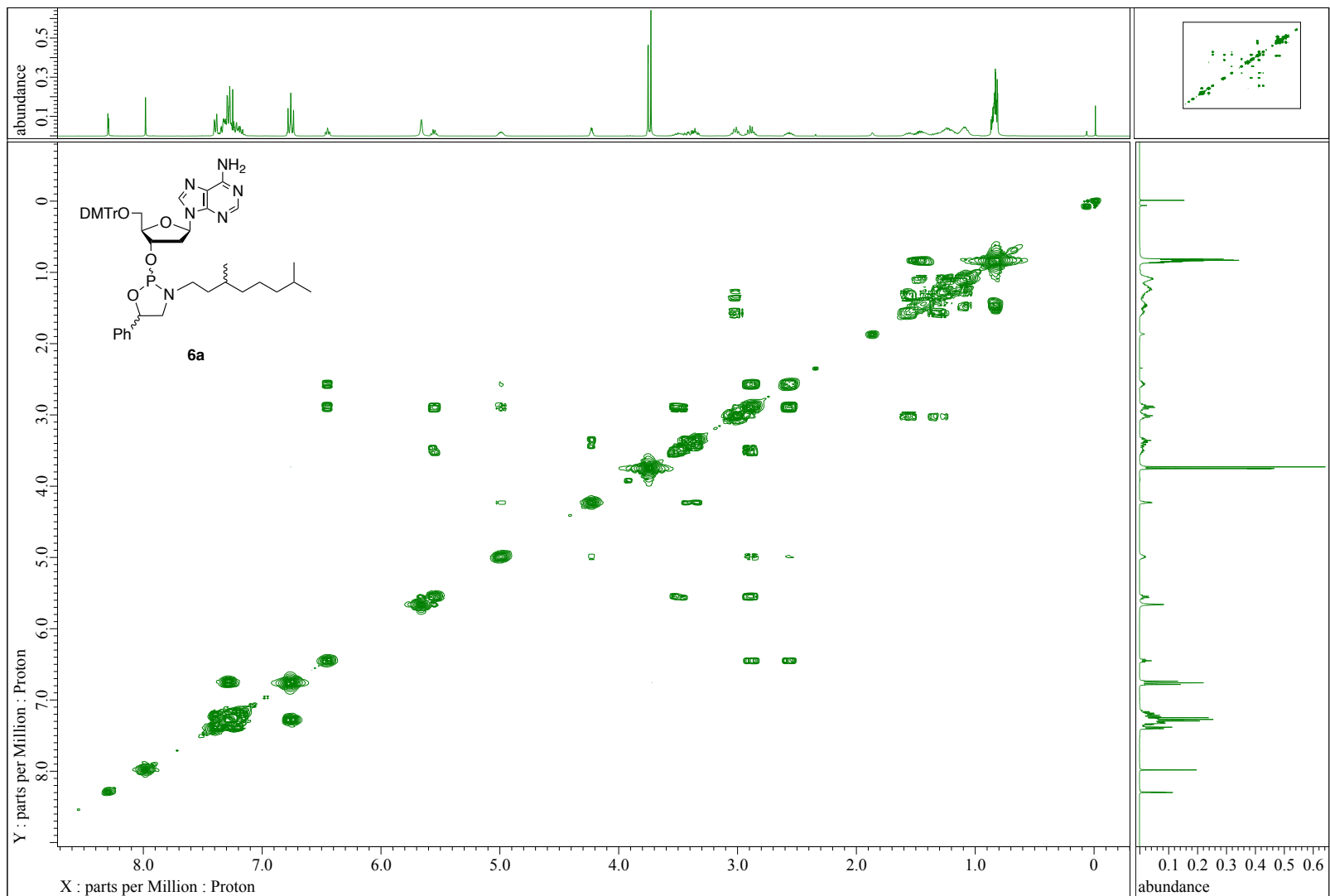
$^{13}\text{C}$   $\{^1\text{H}\}$  NMR (101 MHz,  $\text{CDCl}_3$ )



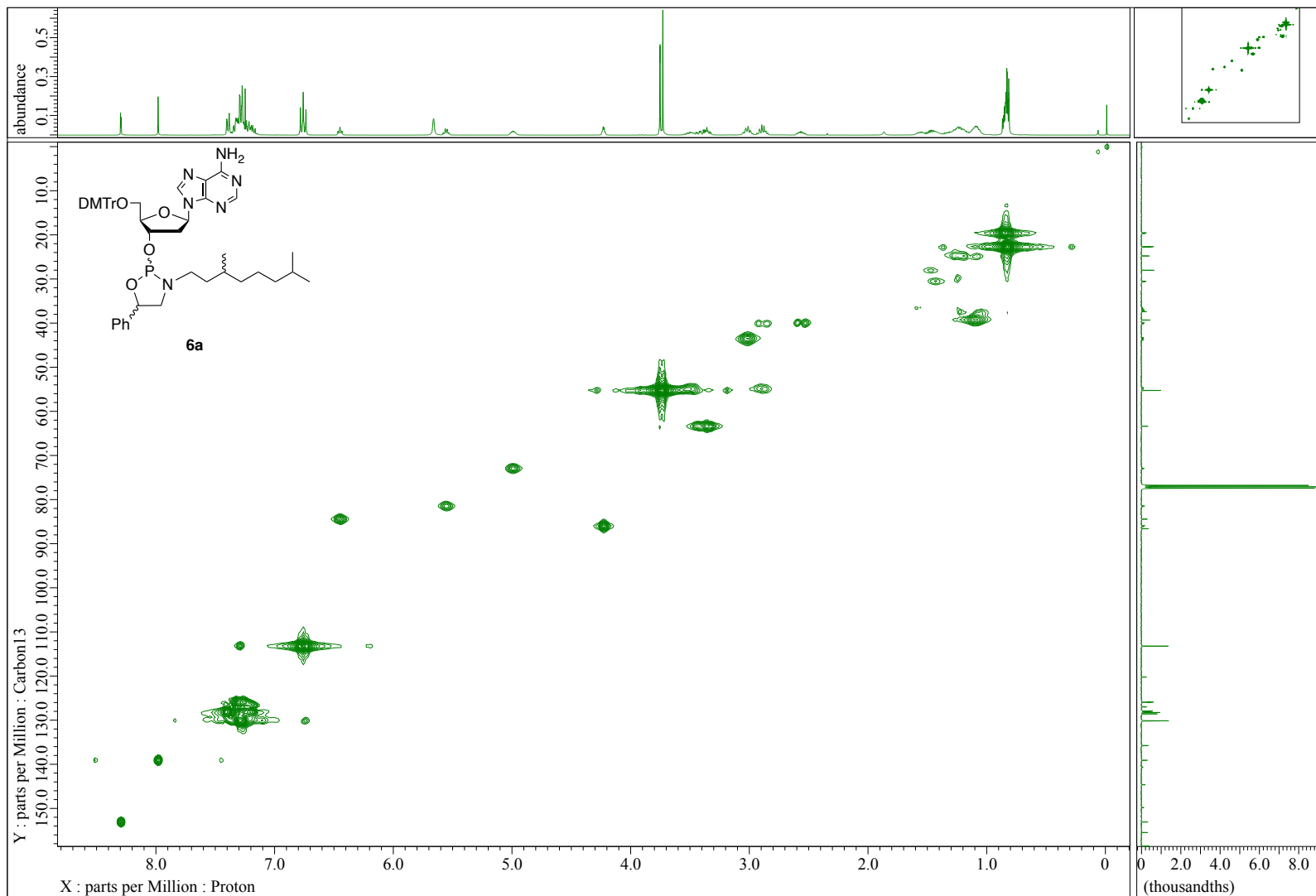
$^{31}\text{P}$   $\{^1\text{H}\}$  NMR (162 MHz,  $\text{CDCl}_3$ )



# COSY (CDCl<sub>3</sub>)



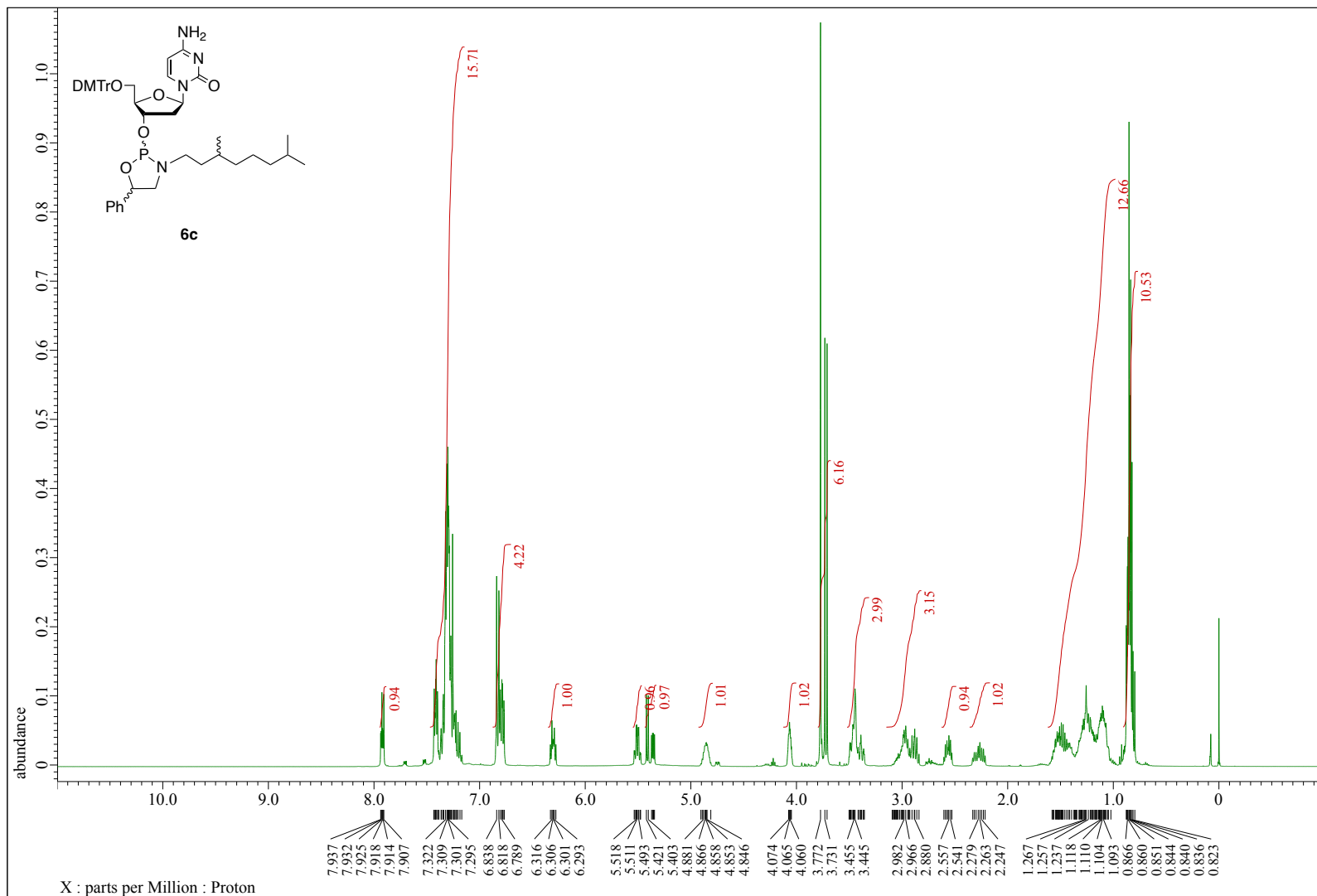
# HMQC (CDCl<sub>3</sub>)



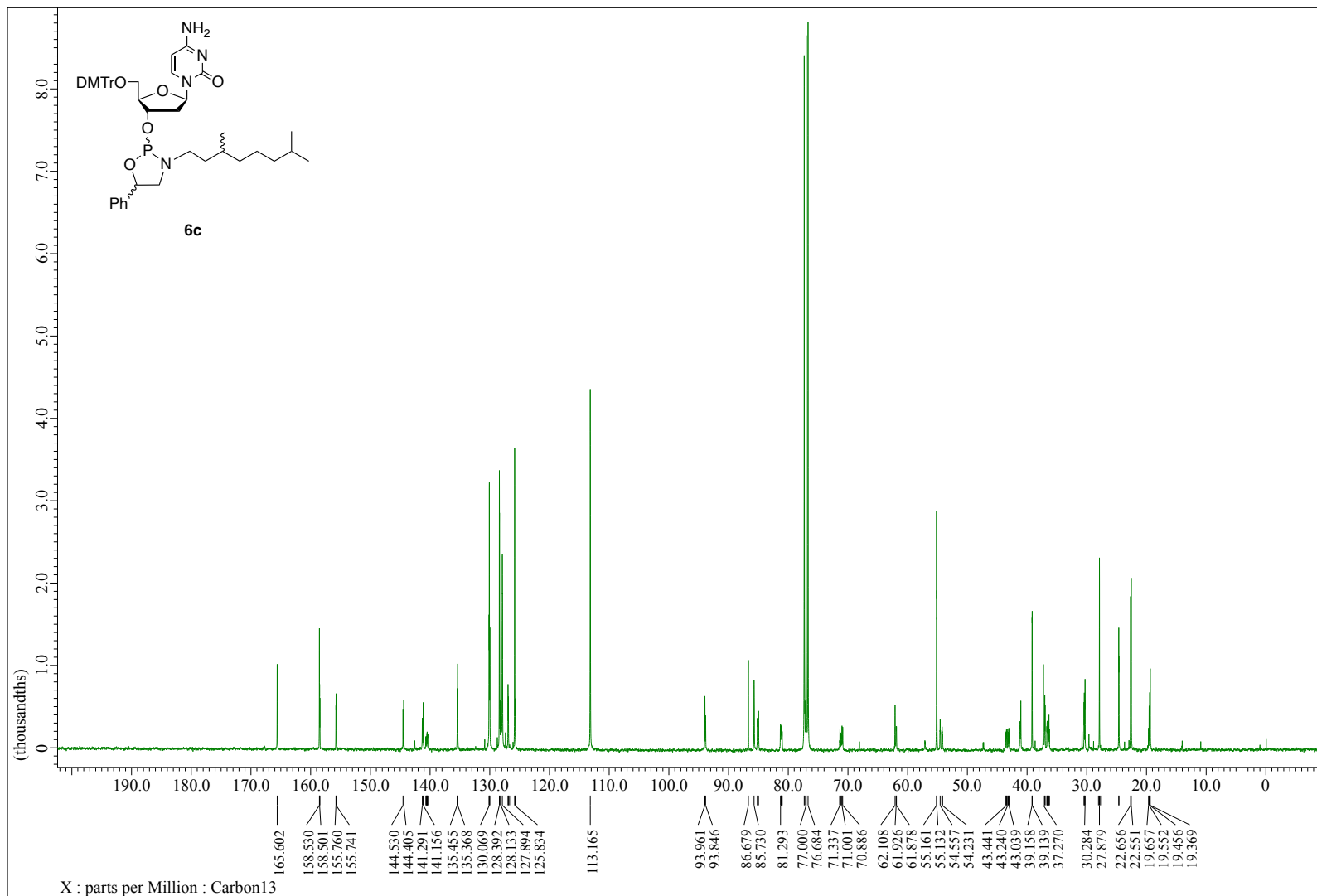




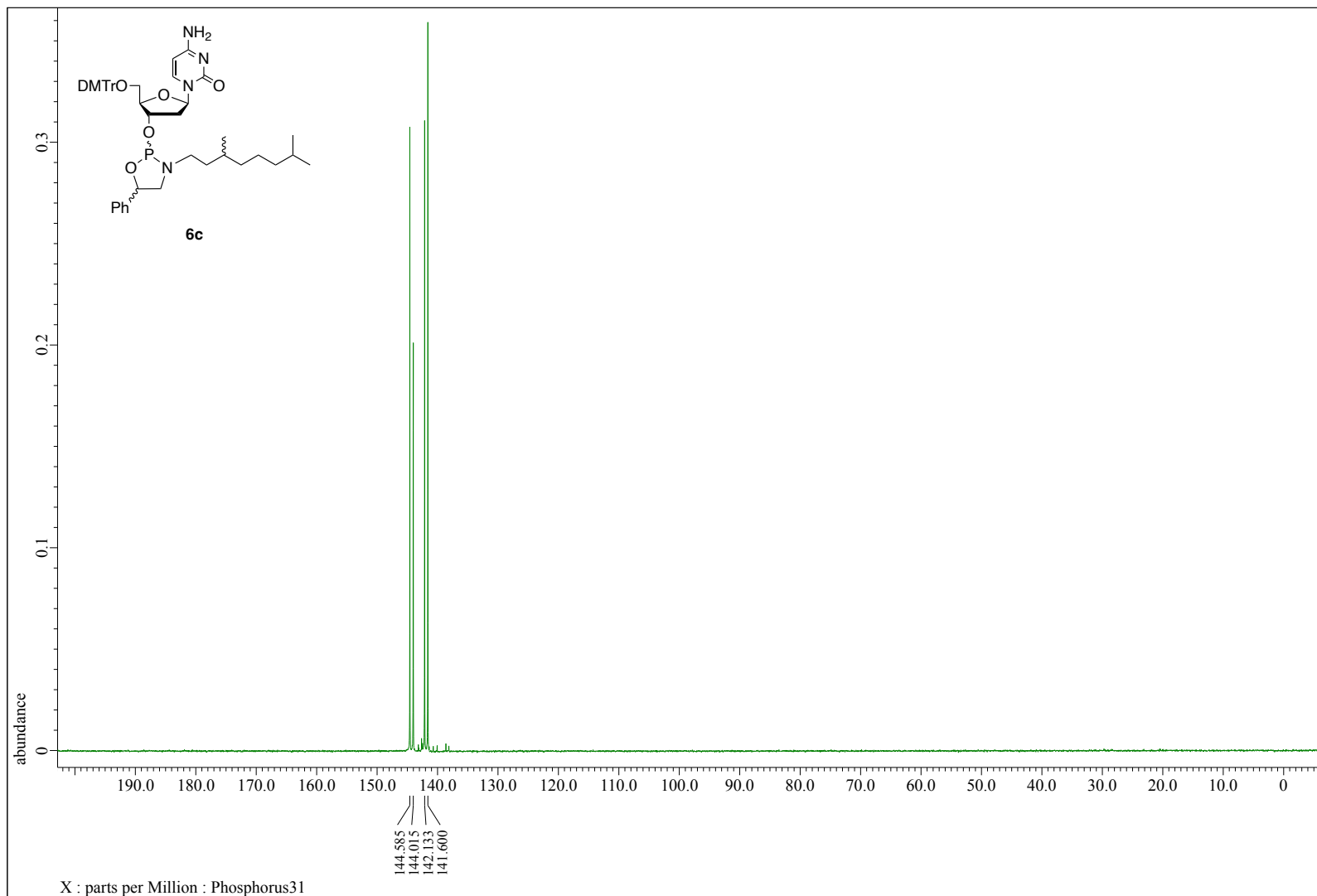
**dCy oxazaphospholidine *N*-Thg monomer (6c)**  
**<sup>1</sup>H NMR (400 MHz, CDCl<sub>3</sub>)**



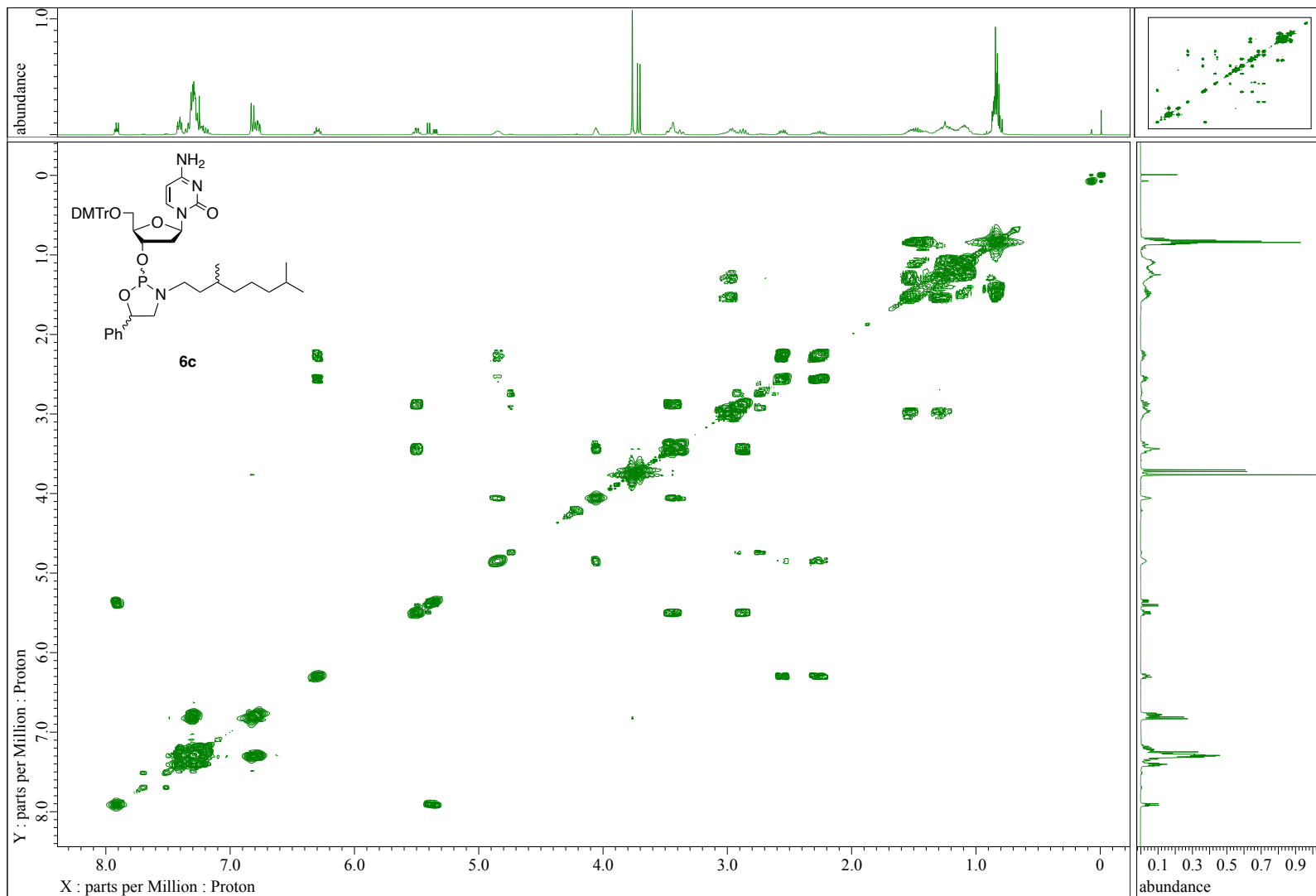
$^{13}\text{C}$   $\{^1\text{H}\}$  NMR (101 MHz,  $\text{CDCl}_3$ )



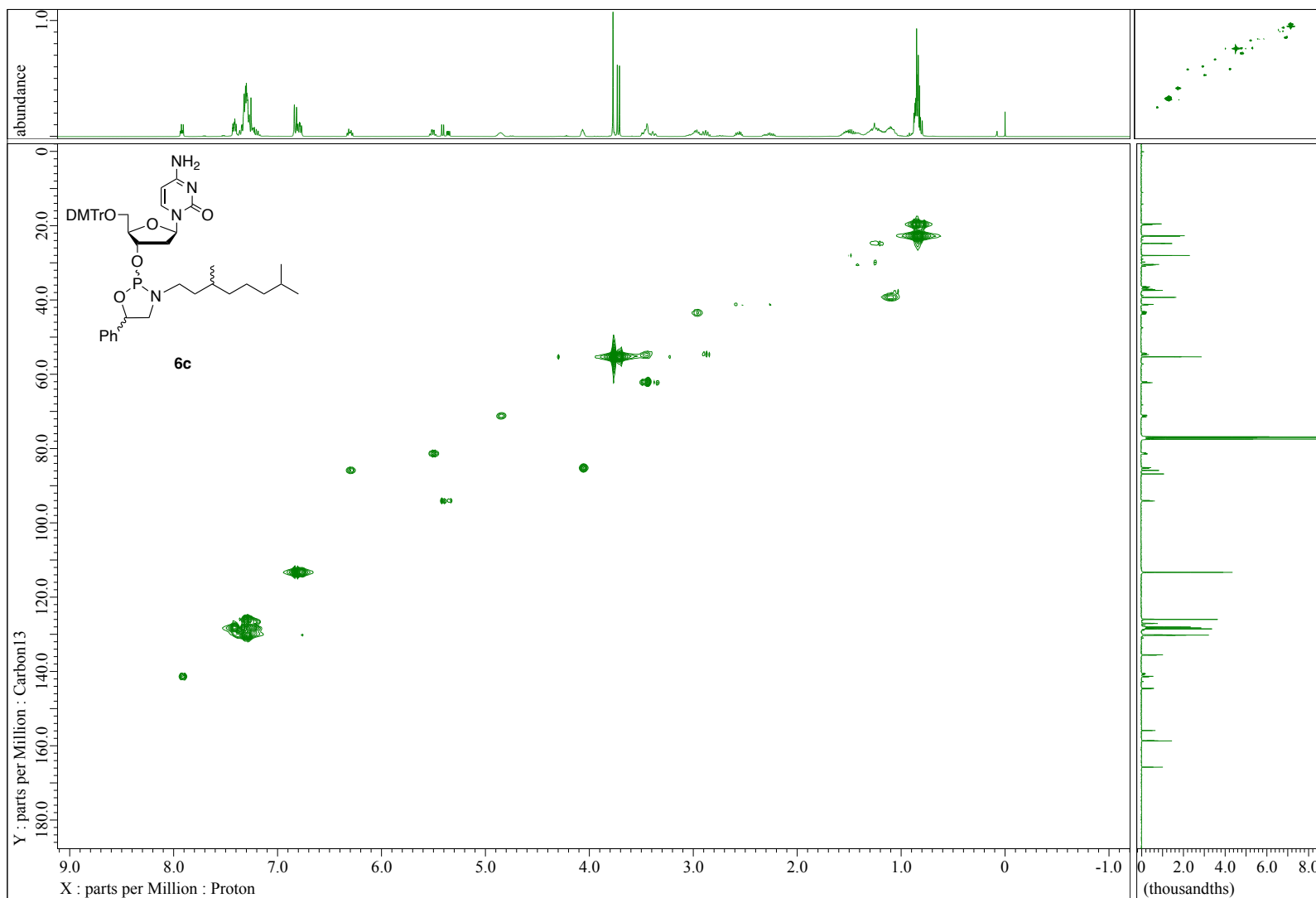
$^{31}\text{P}$   $\{^1\text{H}\}$  NMR (162 MHz,  $\text{CDCl}_3$ )



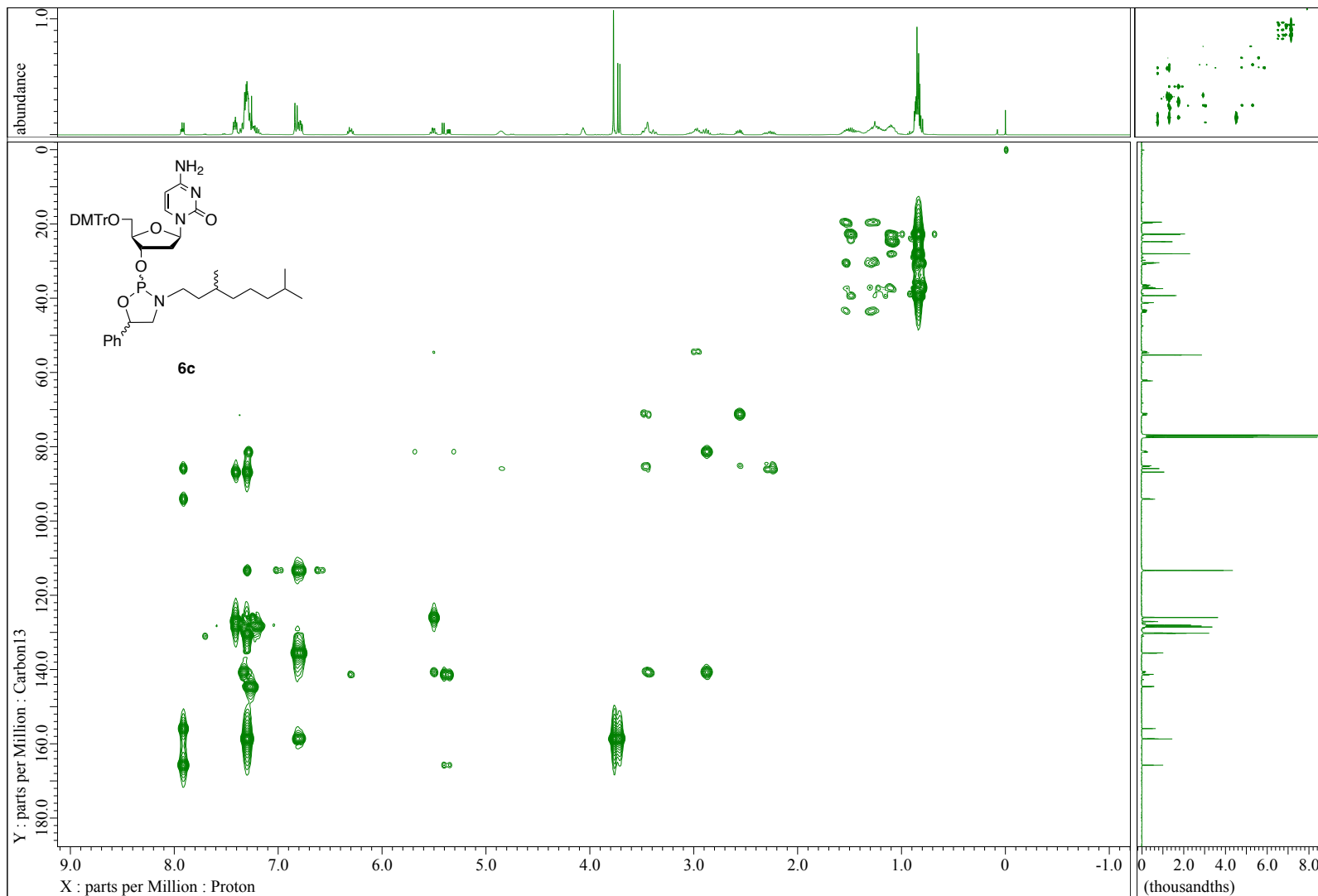
COSY (CDCl<sub>3</sub>)



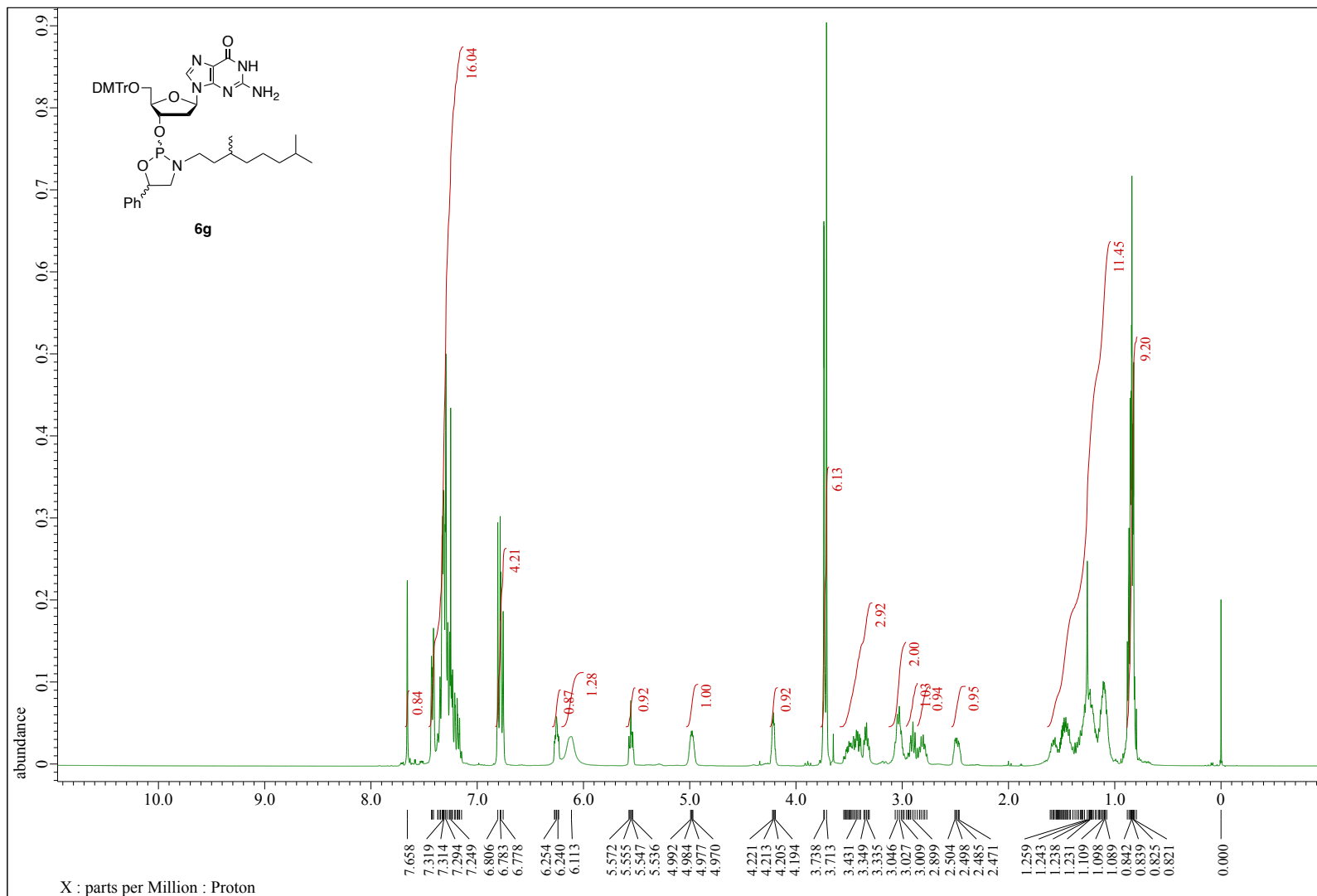
# HMQC (CDCl<sub>3</sub>)



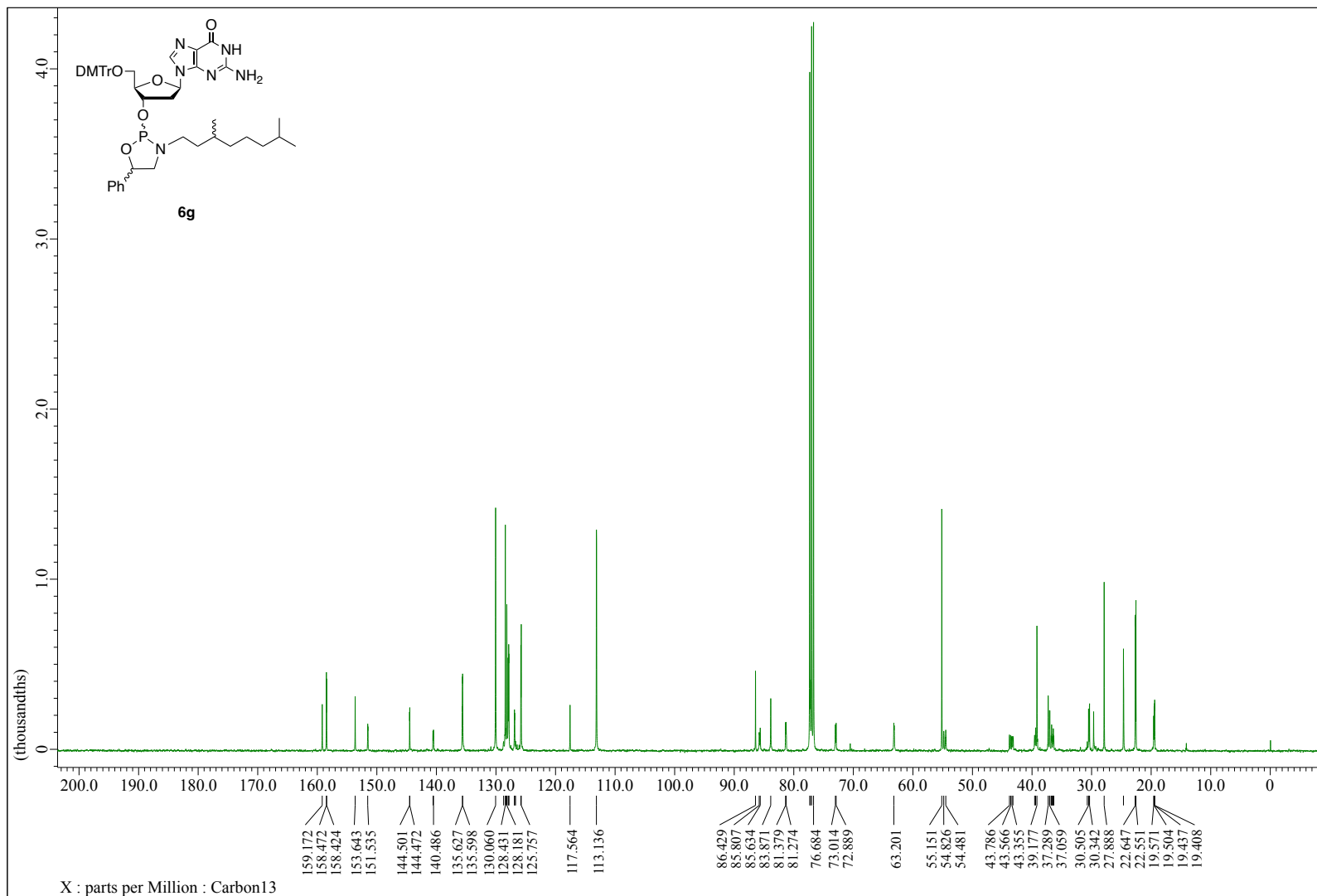
# HMBC (CDCl<sub>3</sub>)



**dGu oxazaphospholidine *N*-Thg monomer (6g)**  
**<sup>1</sup>H NMR (400 MHz, CDCl<sub>3</sub>)**

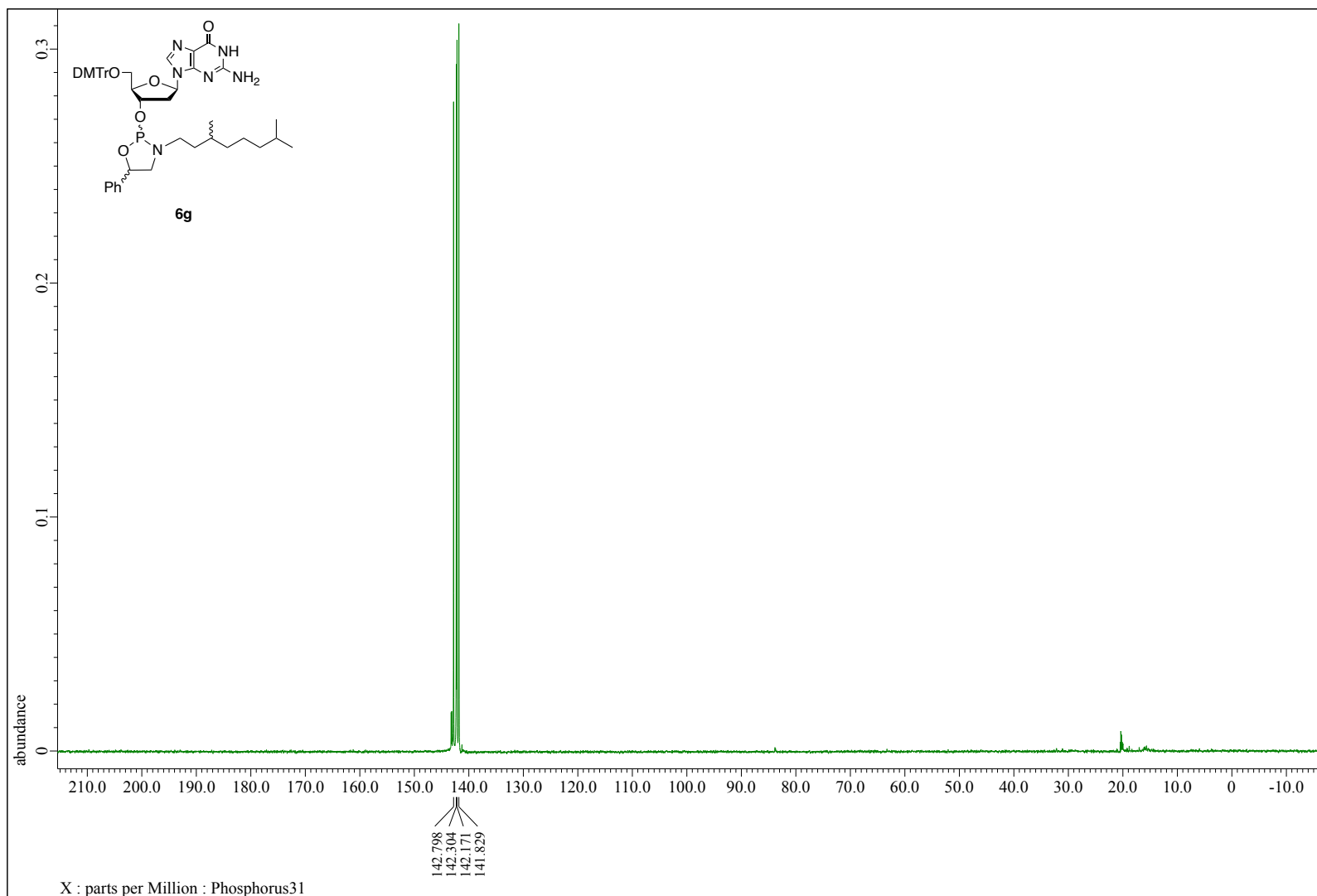


$^{13}\text{C}$   $\{^1\text{H}\}$  NMR (101 MHz,  $\text{CDCl}_3$ )

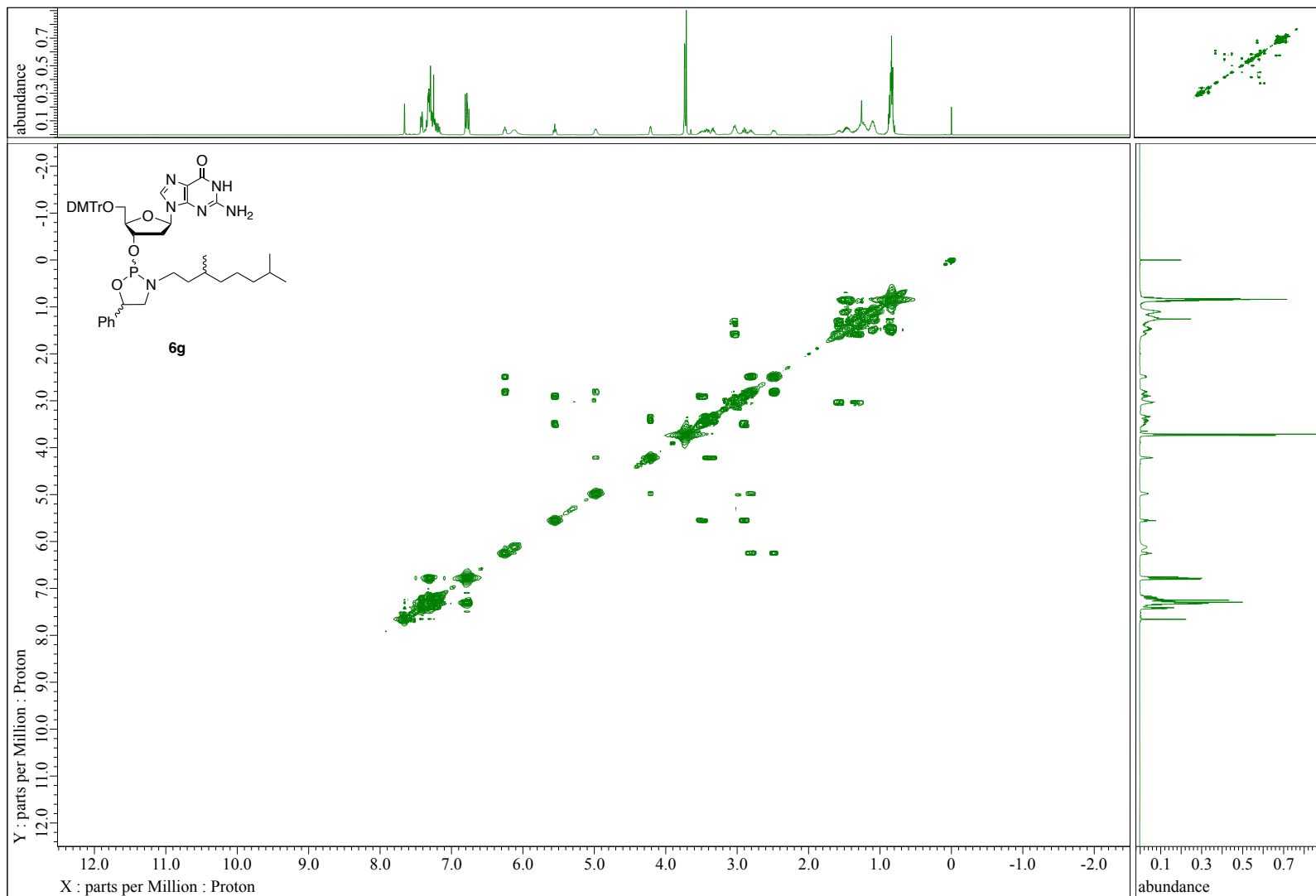




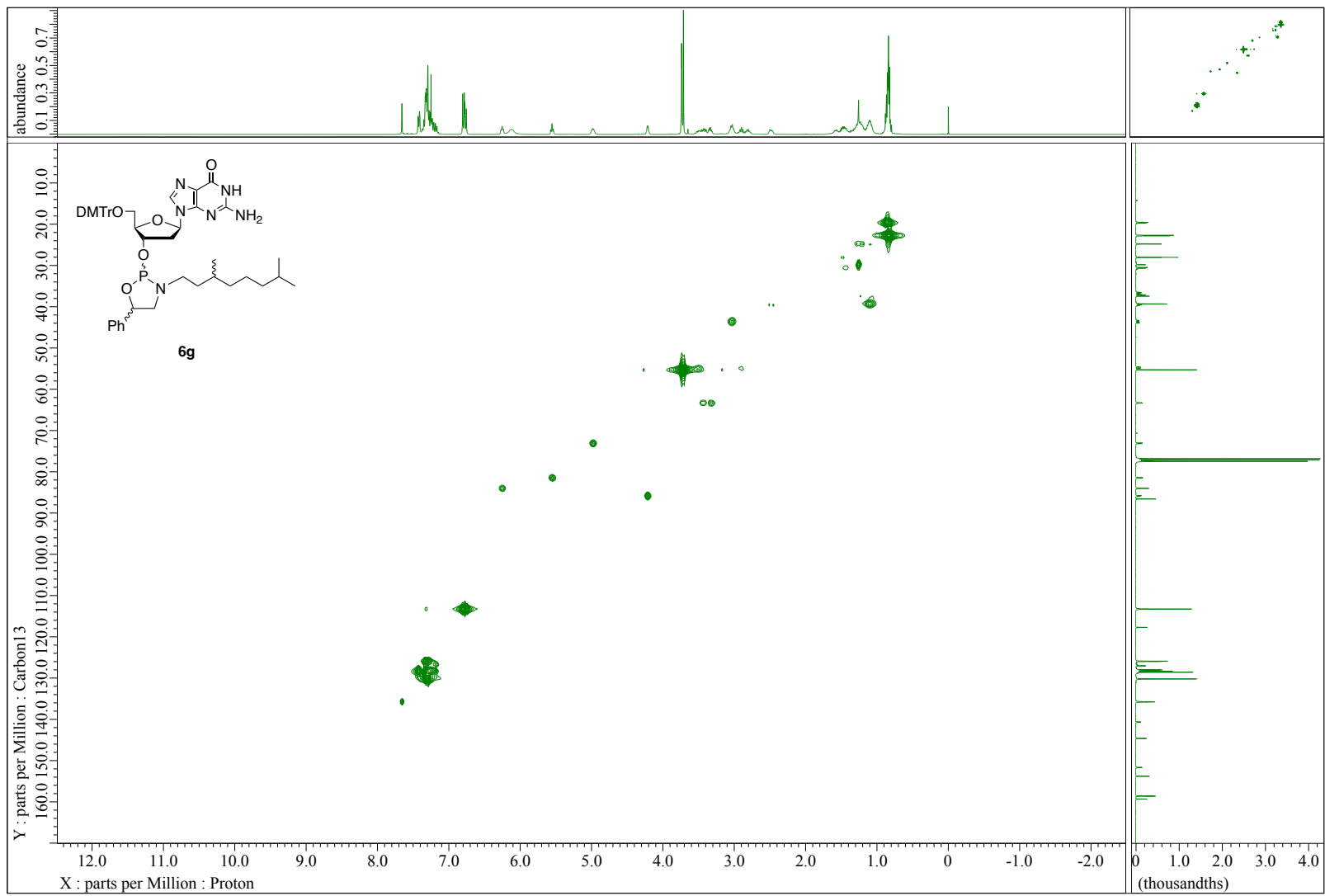
$^{31}\text{P}$   $\{^1\text{H}\}$  NMR (162 MHz,  $\text{CDCl}_3$ )



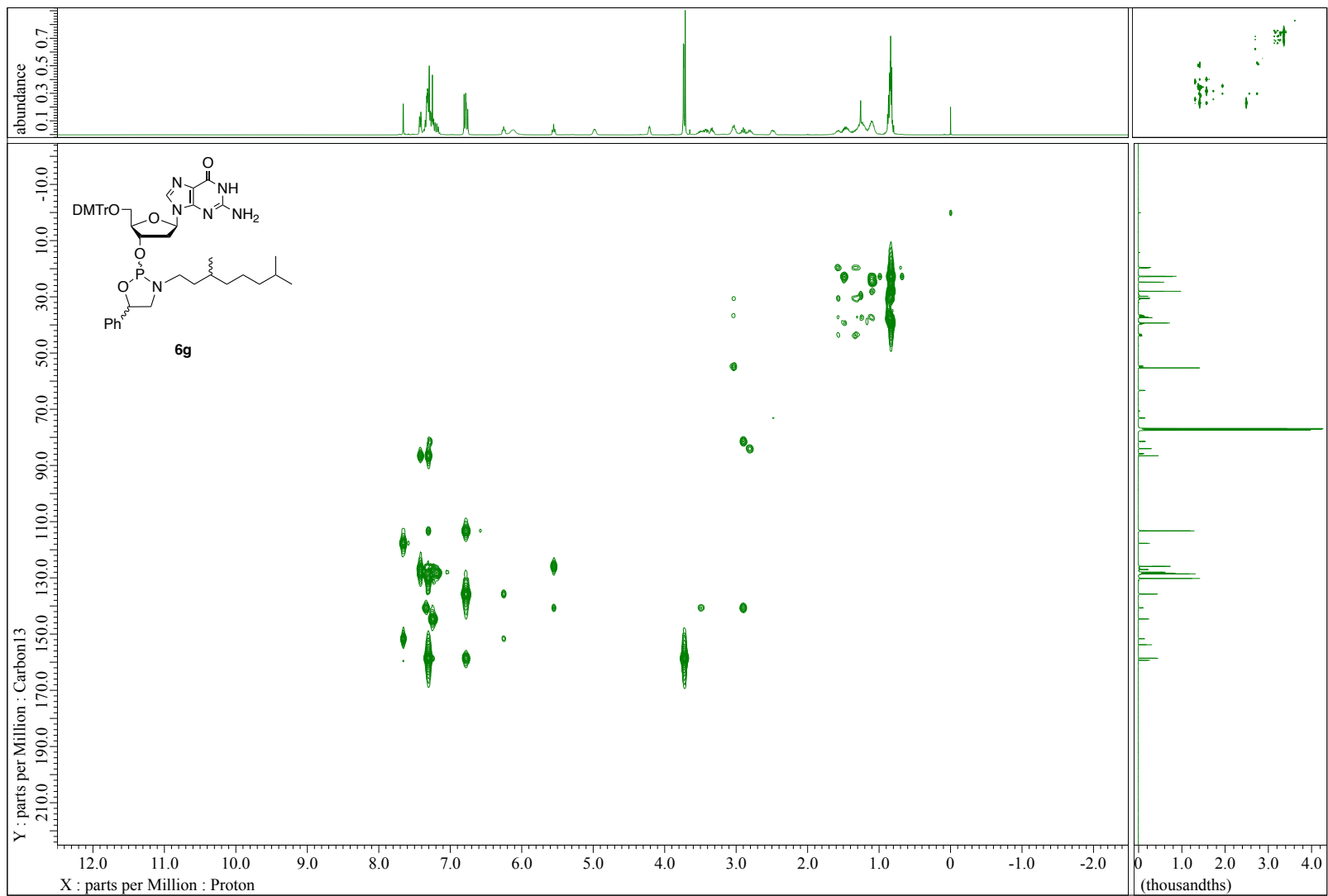
# COSY (CDCl<sub>3</sub>)



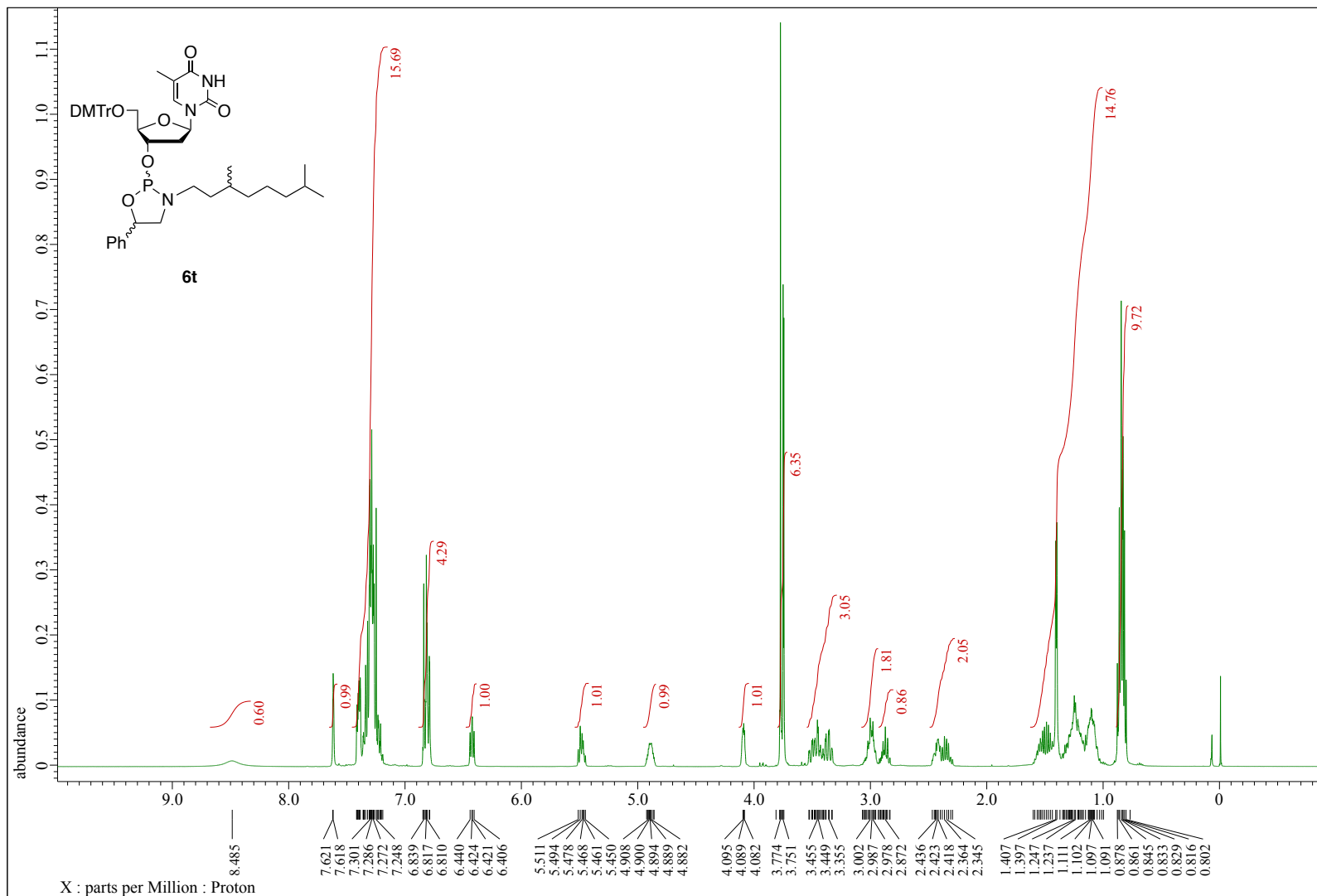
# HMQC (CDCl<sub>3</sub>)



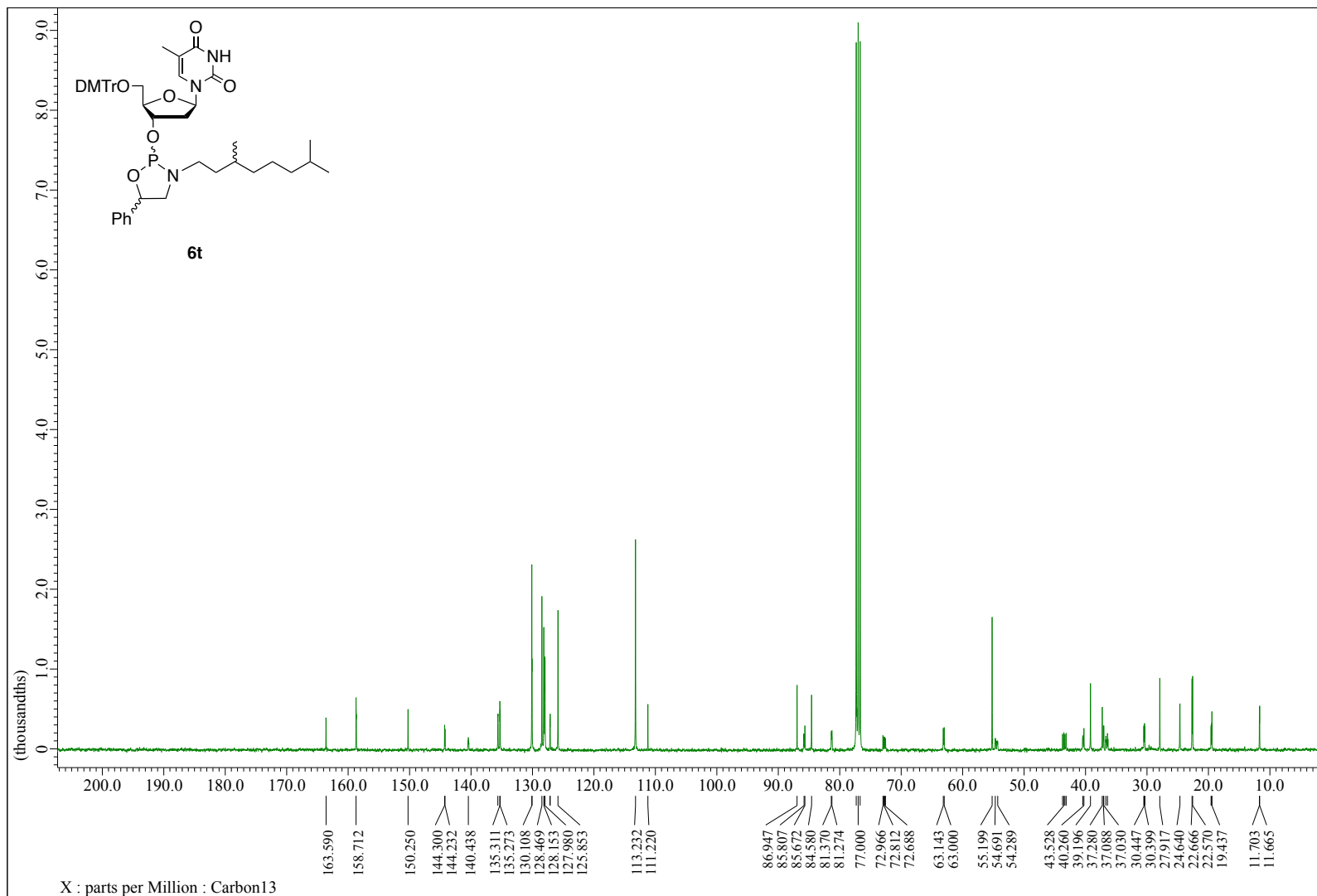
# HMBC (CDCl<sub>3</sub>)



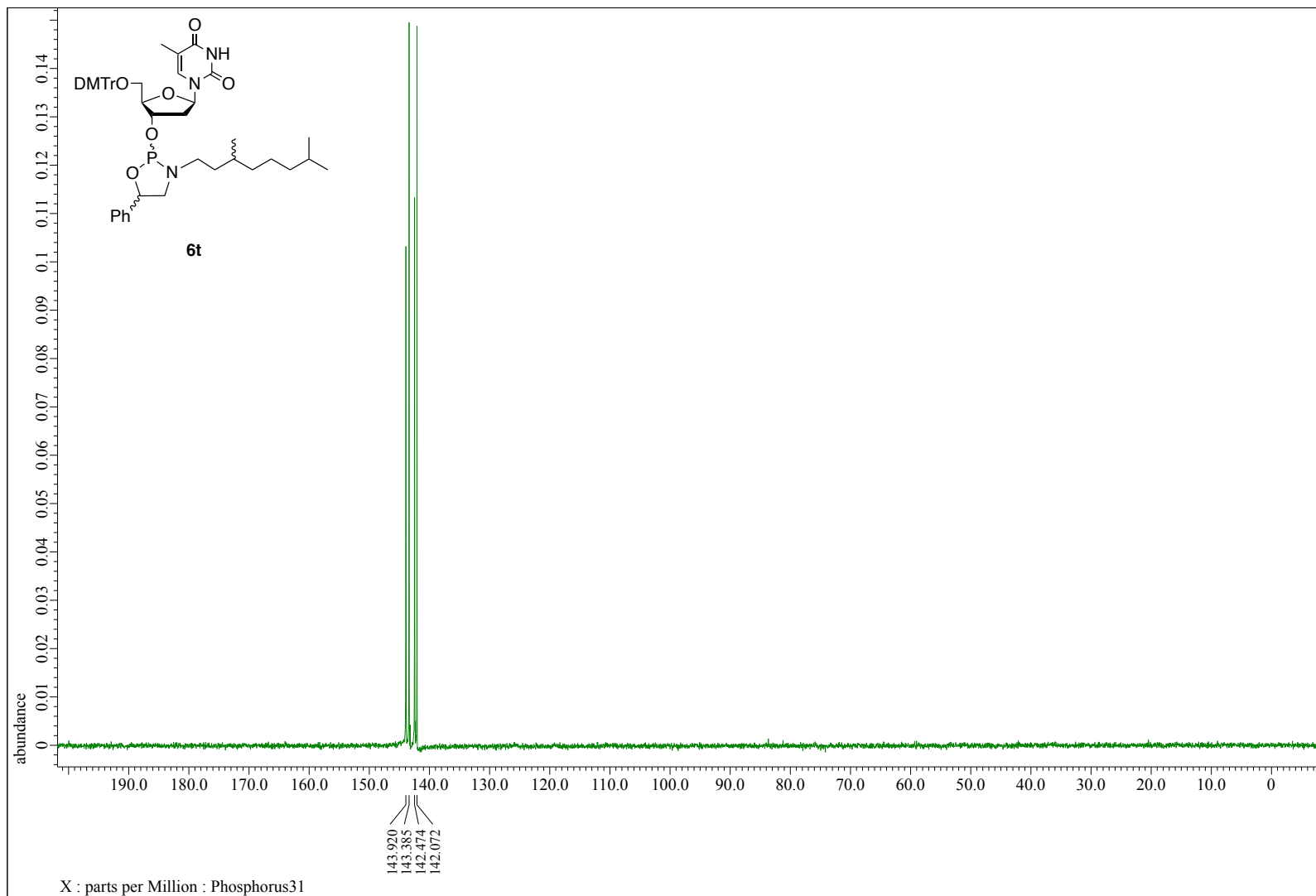
**Th oxazaphospholidine *N*-Thg monomer (6t)**  
<sup>1</sup>H NMR (400 MHz, CDCl<sub>3</sub>)



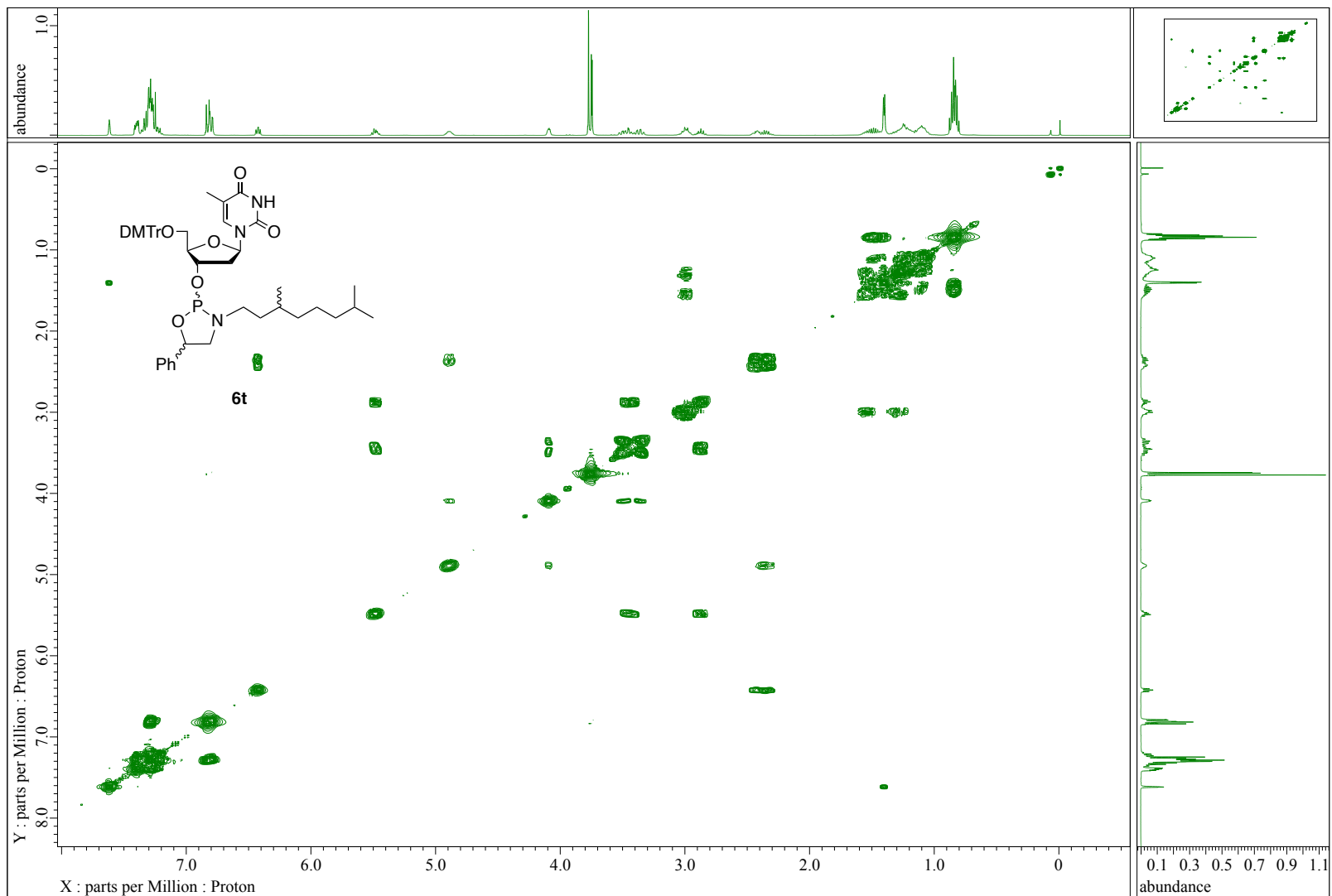
$^{13}\text{C}$   $\{^1\text{H}\}$  NMR (101 MHz,  $\text{CDCl}_3$ )



$^{31}\text{P}$   $\{^1\text{H}\}$  NMR (162 MHz,  $\text{CDCl}_3$ )

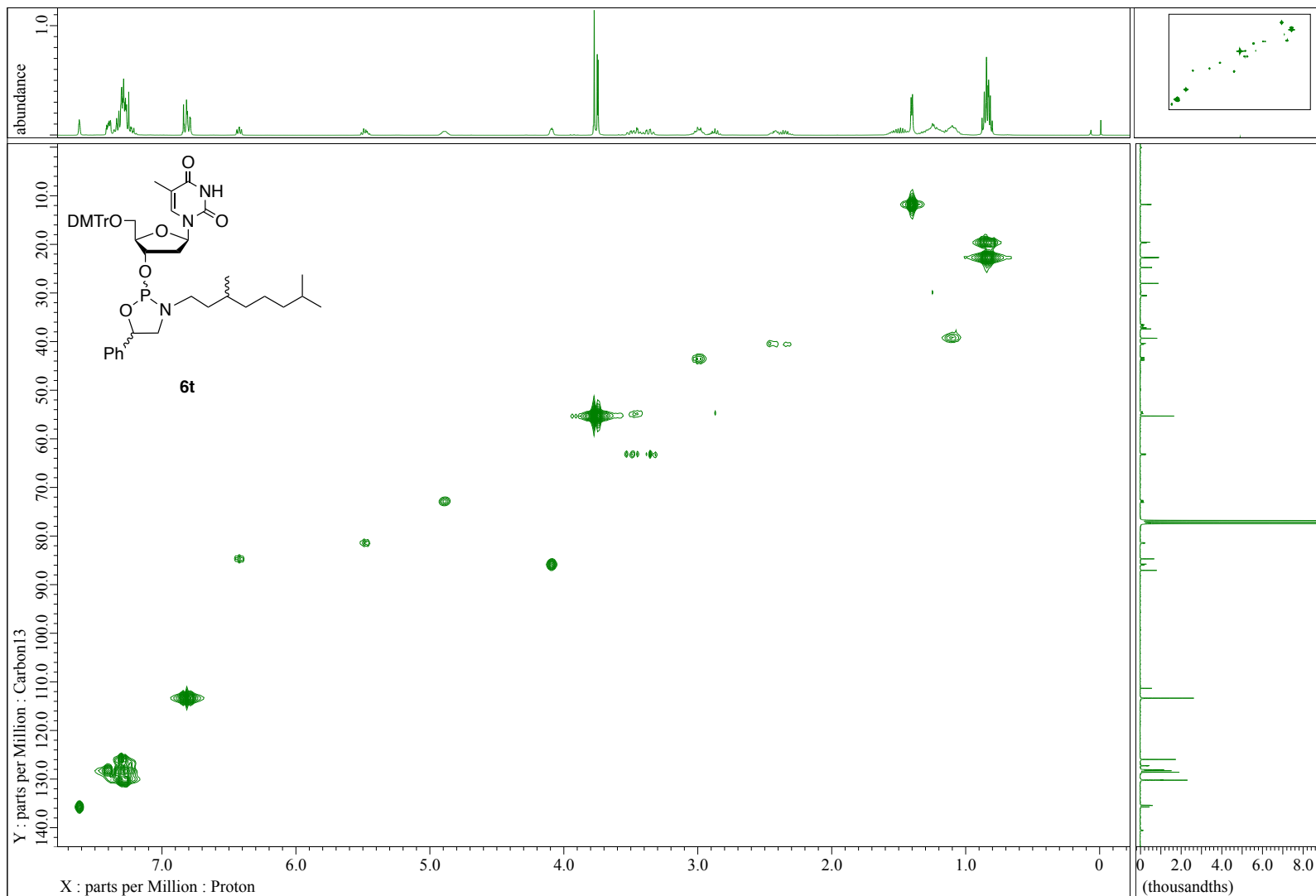


COSY (CDCl<sub>3</sub>)

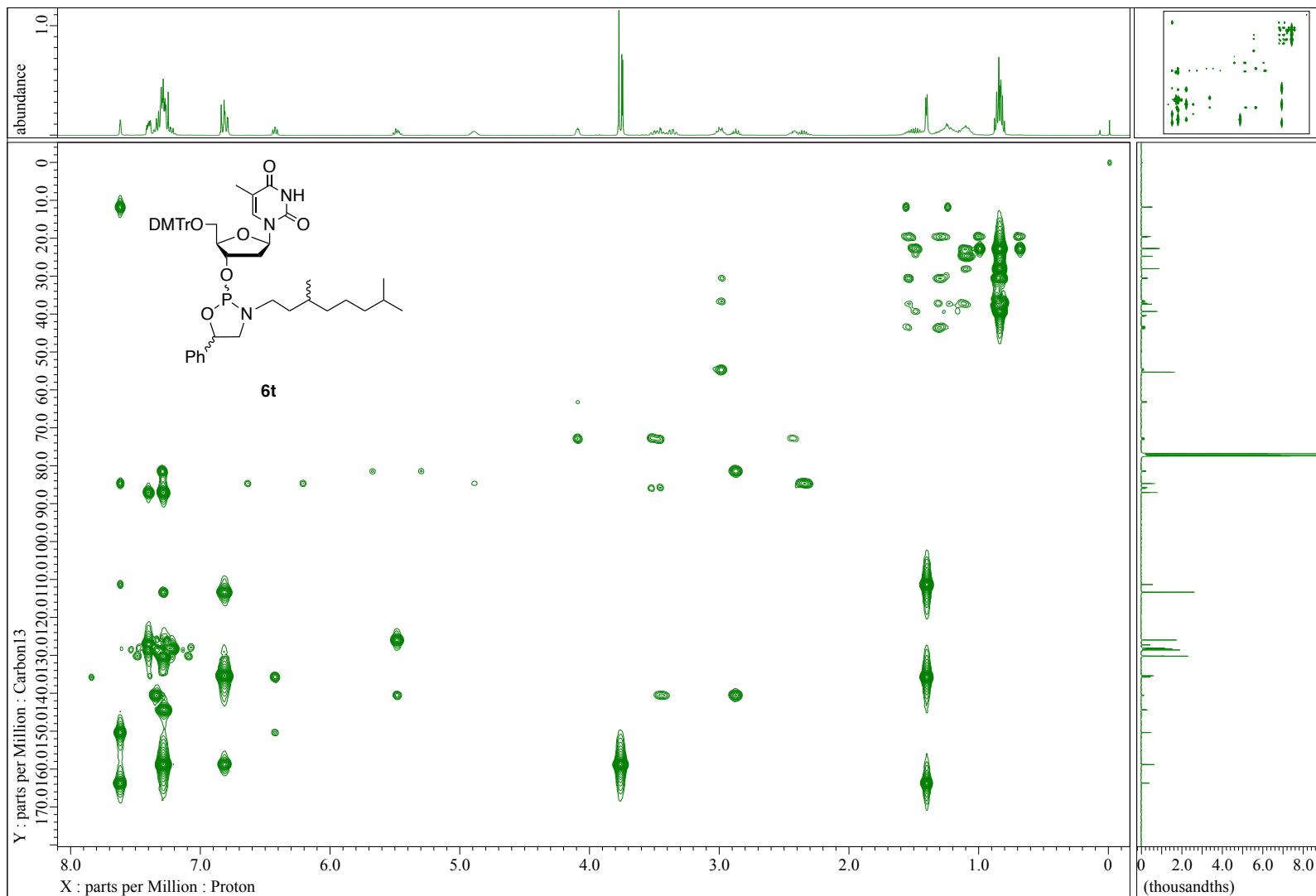




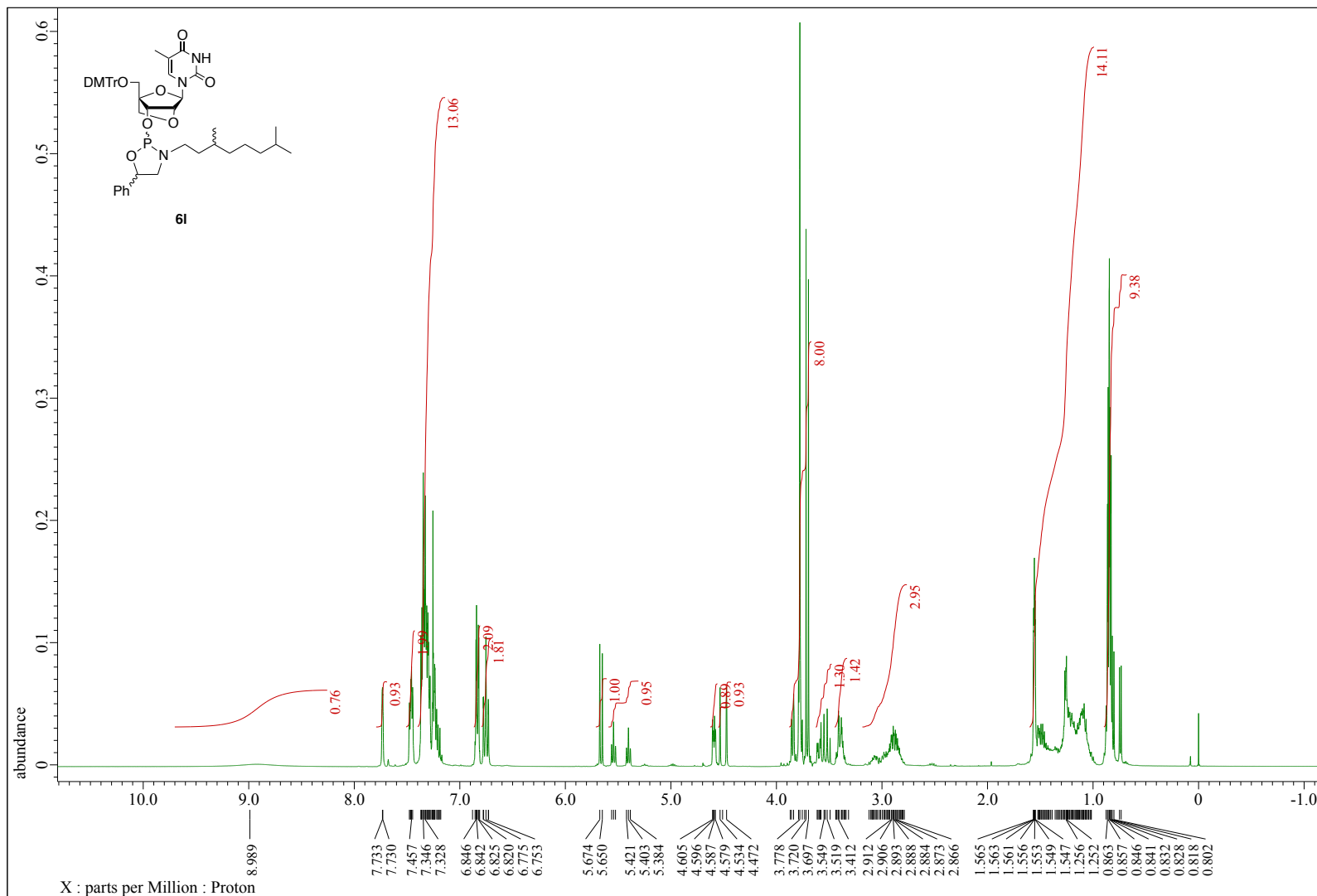
# HMQC (CDCl<sub>3</sub>)



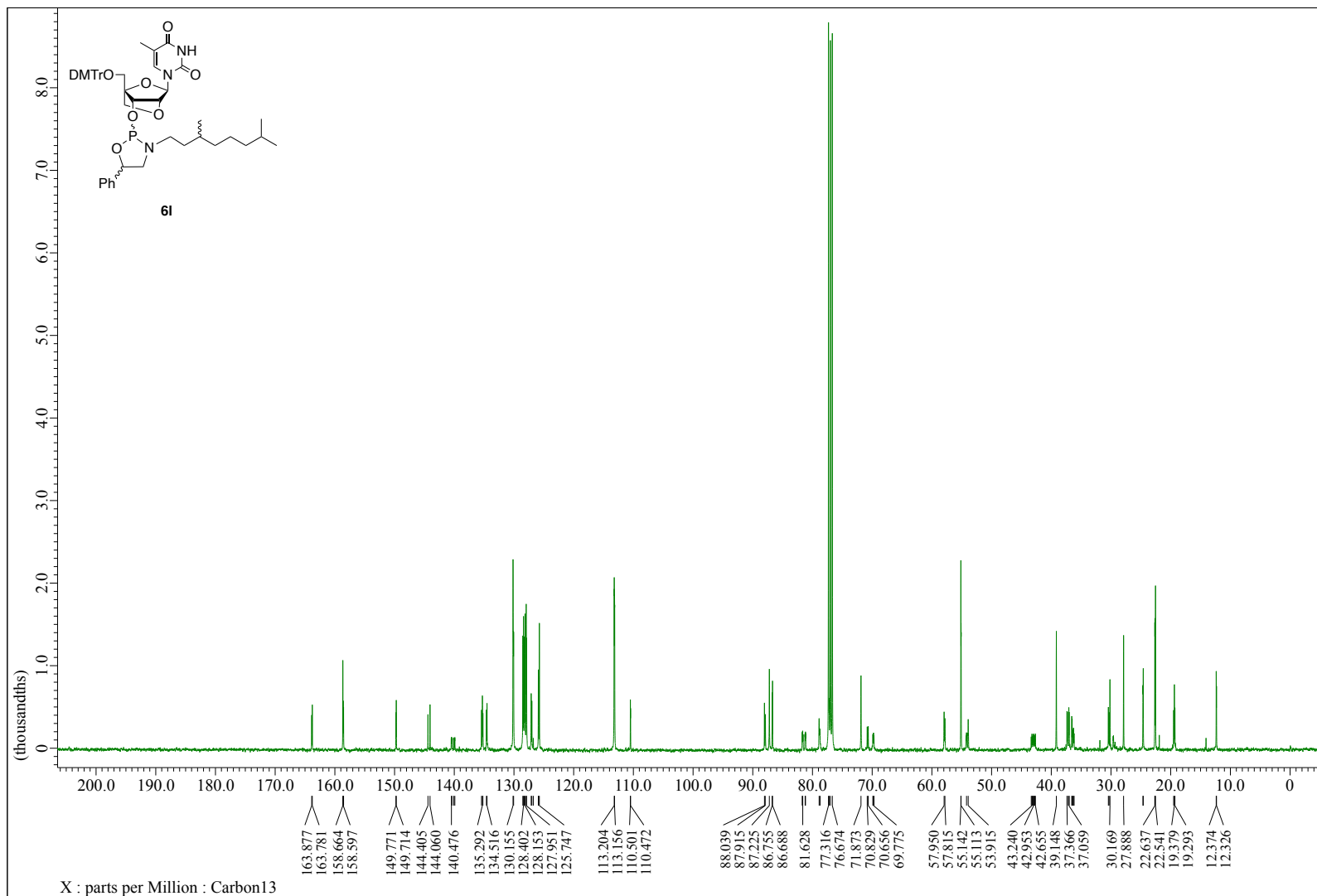
# HMBC (CDCl<sub>3</sub>)



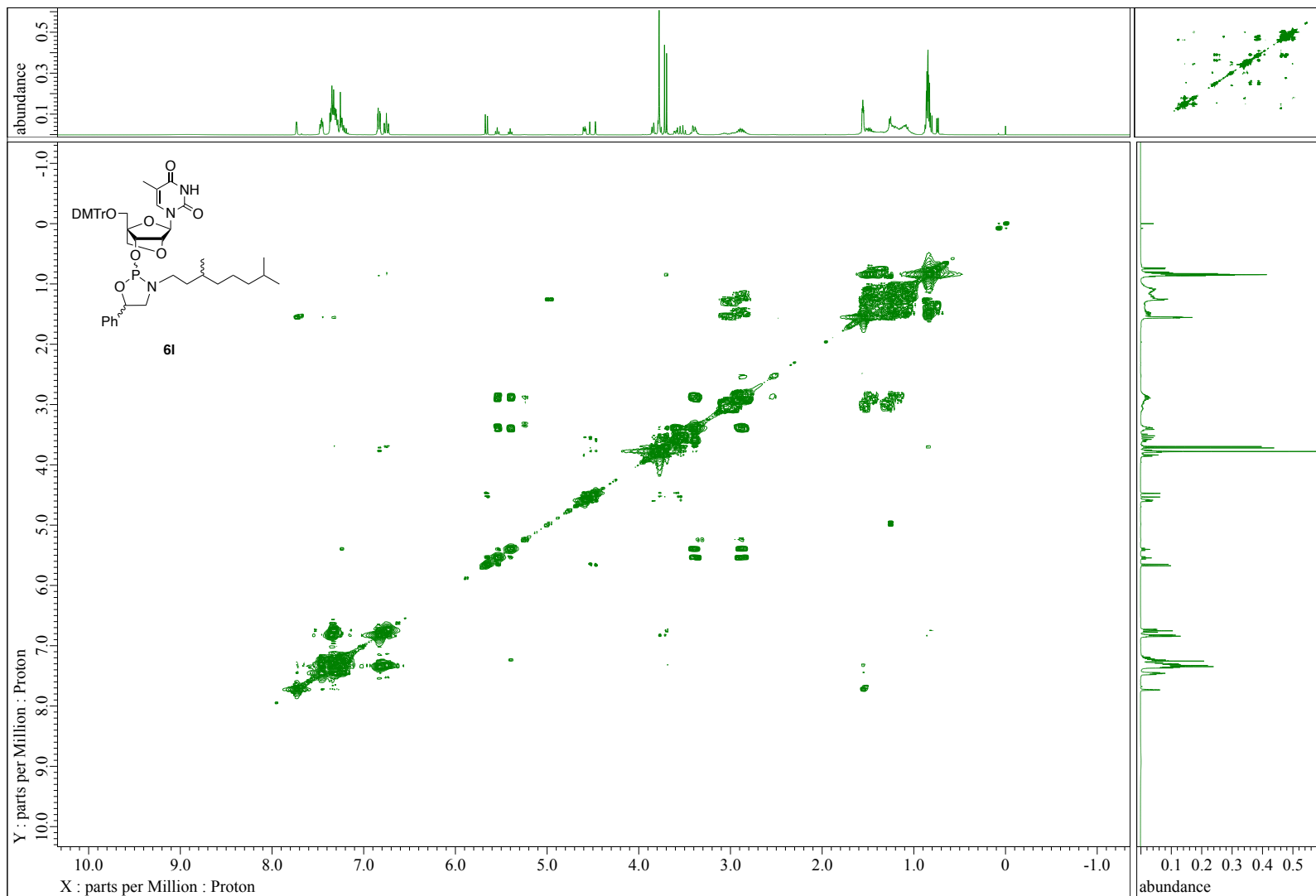
LNATh oxazaphospholidine *N*-Thg monomer (**6l**)  
<sup>1</sup>H NMR (400 MHz, CDCl<sub>3</sub>)



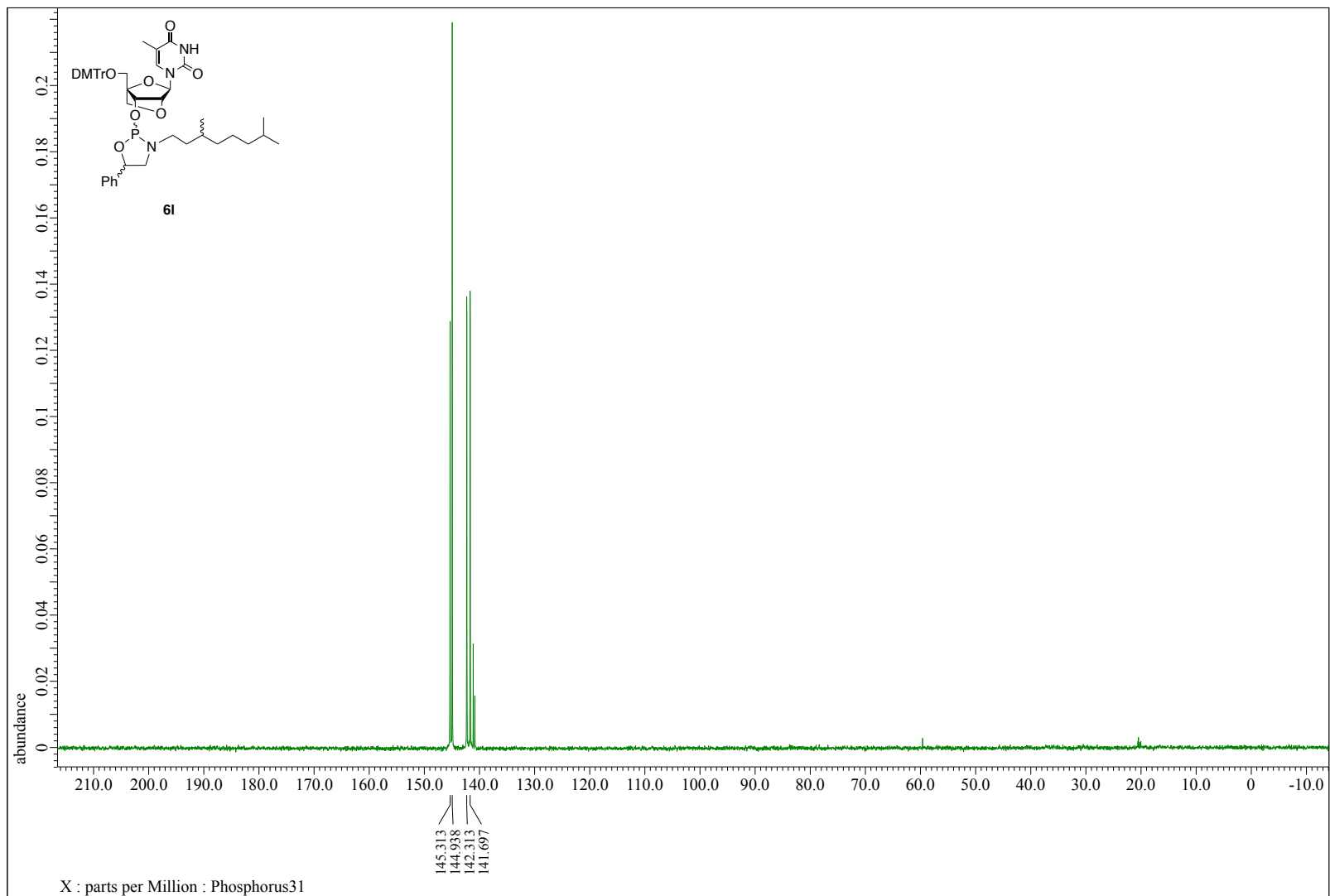
$^{13}\text{C}$   $\{^1\text{H}\}$  NMR (101 MHz,  $\text{CDCl}_3$ )



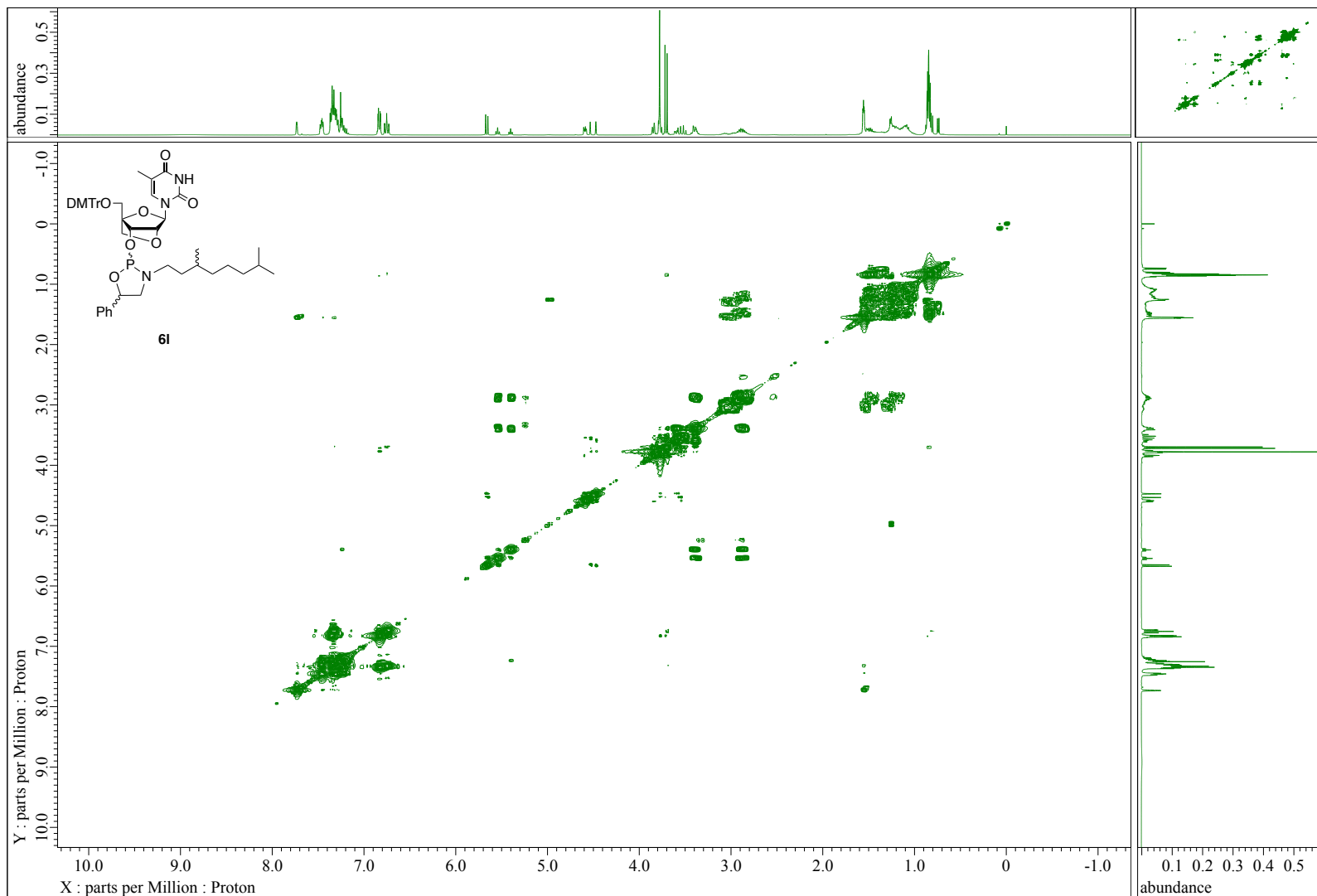
# COSY (CDCl<sub>3</sub>)



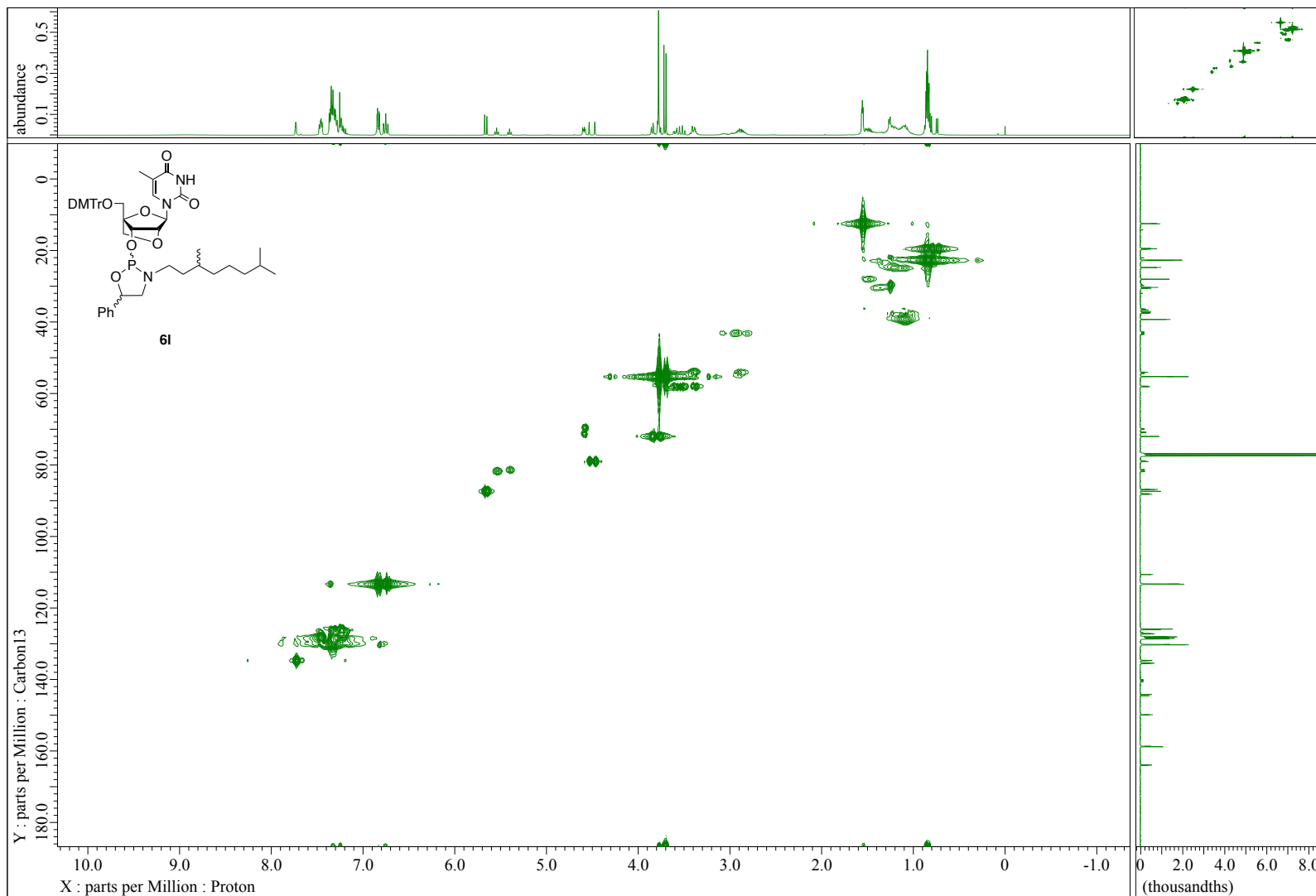
$^{31}\text{P}$   $\{^1\text{H}\}$  NMR (162 MHz,  $\text{CDCl}_3$ )



COSY (CDCl<sub>3</sub>)

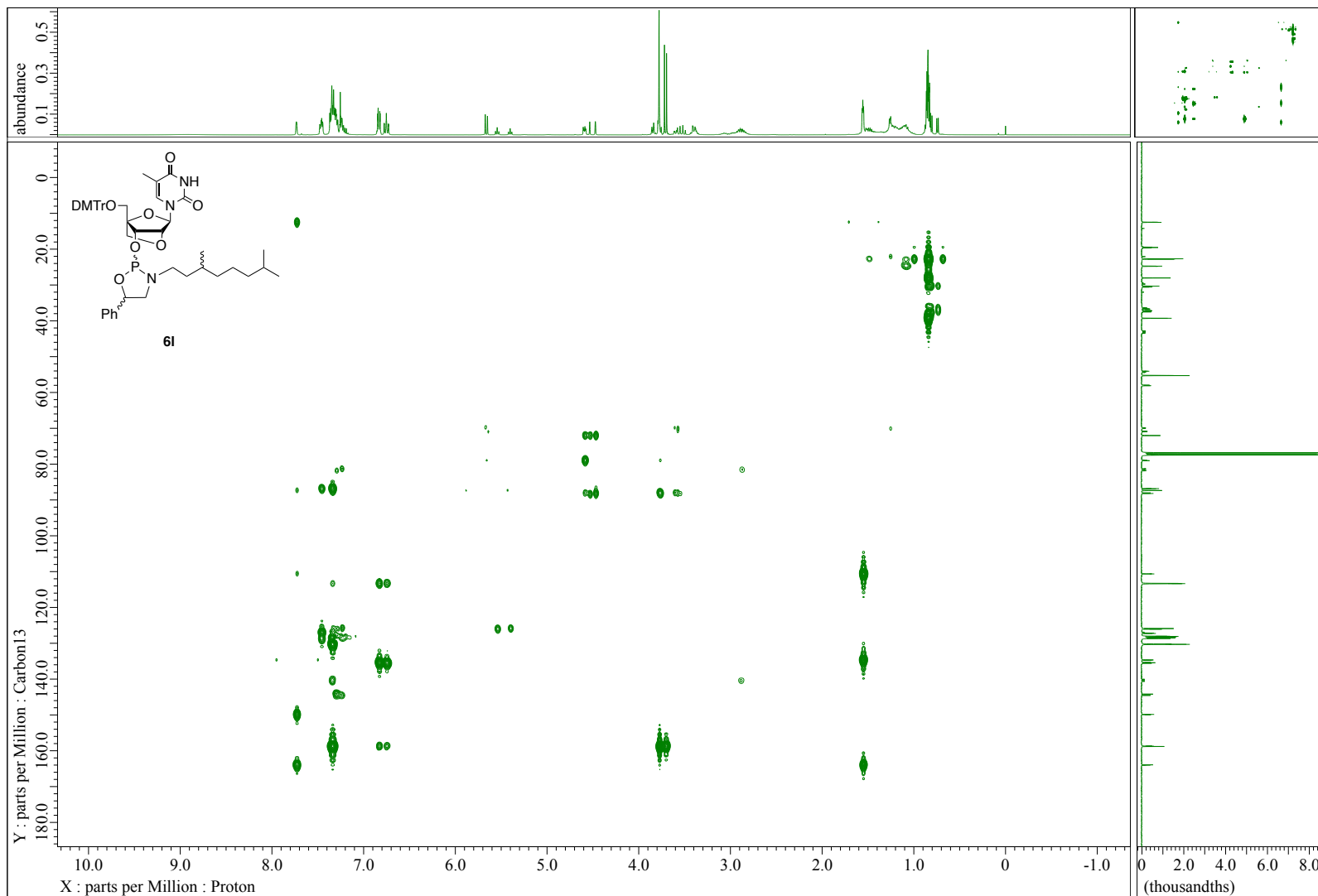


# HMQC (CDCl<sub>3</sub>)





# HMBC (CDCl<sub>3</sub>)



PO-DNA dodecamer d(C<sub>P</sub>O A<sub>P</sub>O G<sub>P</sub>O T<sub>P</sub>O C<sub>P</sub>O A<sub>P</sub>O G<sub>P</sub>O T<sub>P</sub>O C<sub>P</sub>O A<sub>P</sub>O)T **11**  
<sup>1</sup>H NMR (500 MHz, D<sub>2</sub>O)

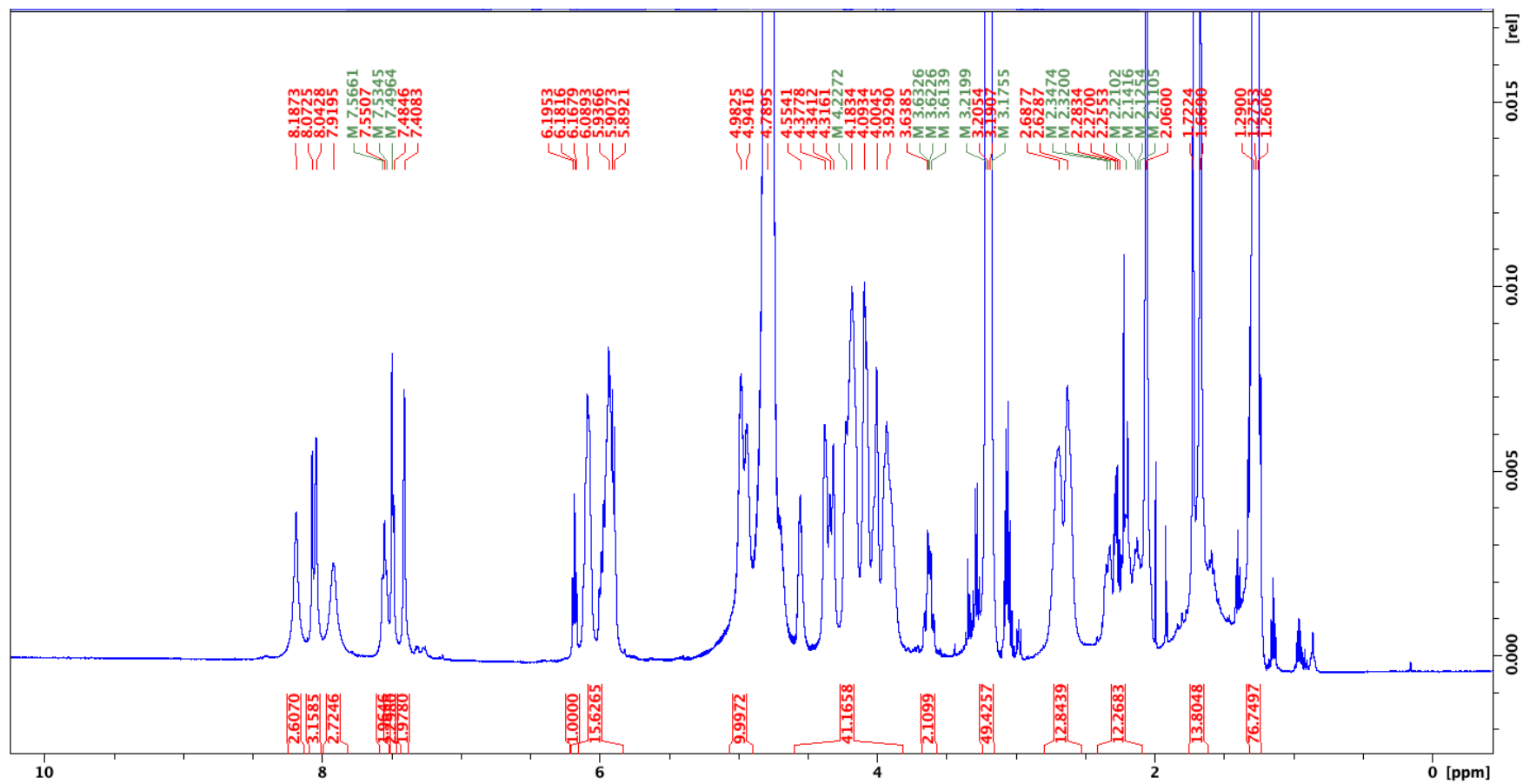


Figure S7 <sup>1</sup>H NMR spectra of PO-DNA dodecamer d(C<sub>P</sub>O A<sub>P</sub>O G<sub>P</sub>O T<sub>P</sub>O C<sub>P</sub>O A<sub>P</sub>O G<sub>P</sub>O T<sub>P</sub>O C<sub>P</sub>O A<sub>P</sub>O)T **11** (500 MHz, D<sub>2</sub>O).

$^{31}\text{P}$   $\{^1\text{H}\}$  NMR (500 MHz,  $\text{D}_2\text{O}$ )

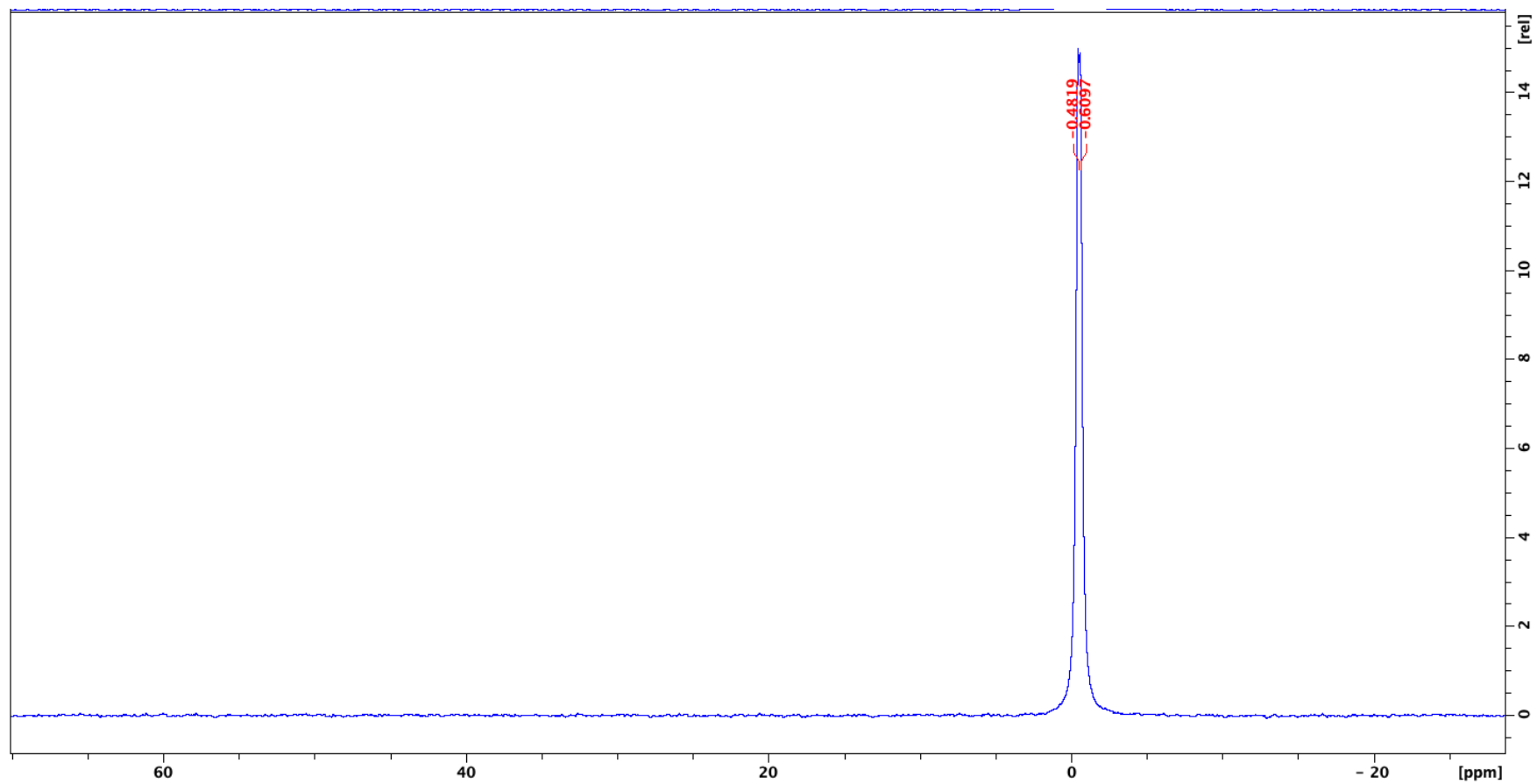
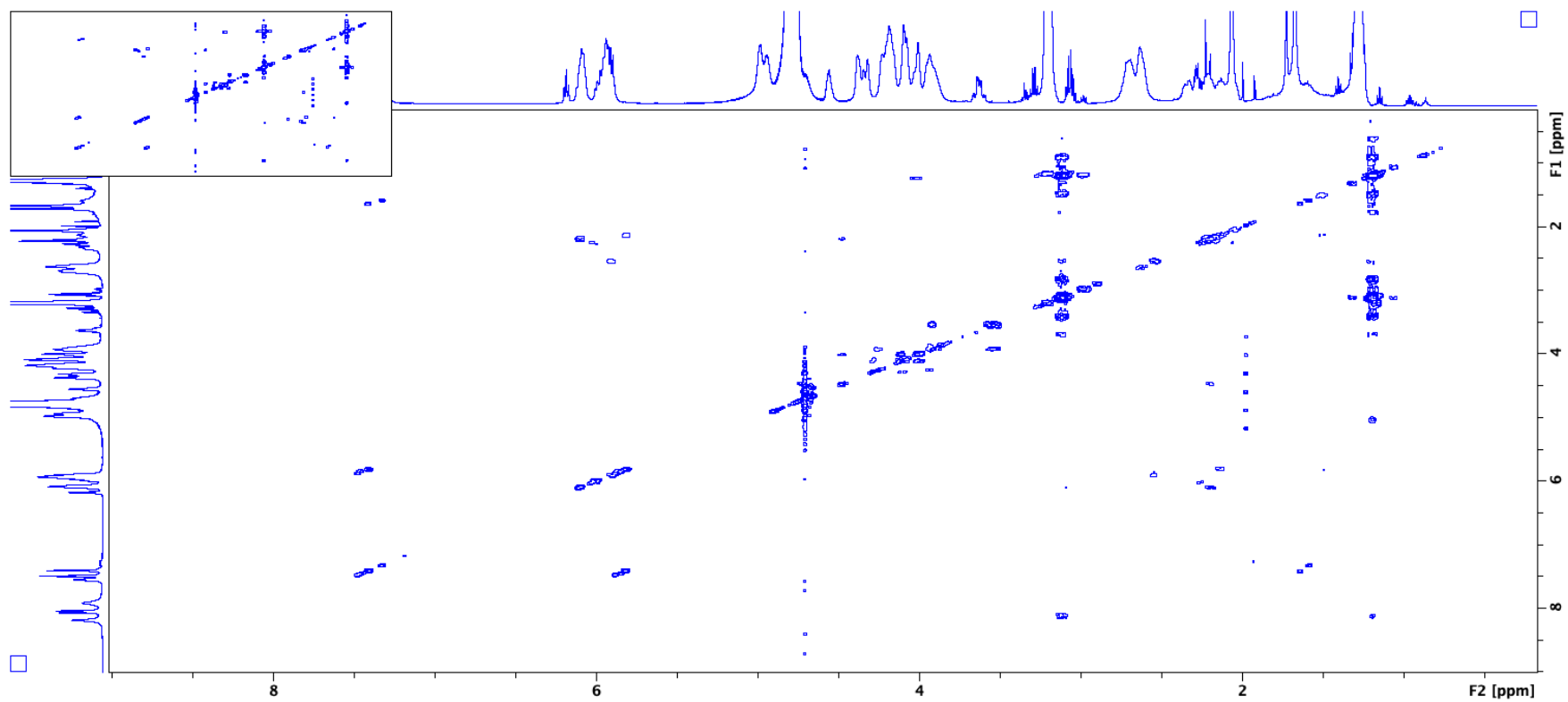


Figure S8  $^{31}\text{P}$  NMR spectra of PO-DNA dodecamer  $\text{d}(\text{C}_{\text{PO}}\text{A}_{\text{PO}}\text{G}_{\text{PO}}\text{T}_{\text{PO}}\text{C}_{\text{PO}}\text{A}_{\text{PO}}\text{G}_{\text{PO}}\text{T}_{\text{PO}}\text{C}_{\text{PO}}\text{A}_{\text{PO}})\text{T}$  **11** (500 MHz,  $\text{D}_2\text{O}$ ).



COSY spectra of PO-DNA dodecamer  $d(C_{PO}A_{PO}G_{PO}T_{PO}C_{PO}A_{PO}G_{PO}T_{PO}C_{PO}A_{PO})T$  **11** (500 MHz,  $D_2O$ ).

PB-DNA tetramer d(C<sub>PB</sub>A<sub>PB</sub>G<sub>PB</sub>T) 16  
<sup>1</sup>H NMR (600 MHz, D<sub>2</sub>O)

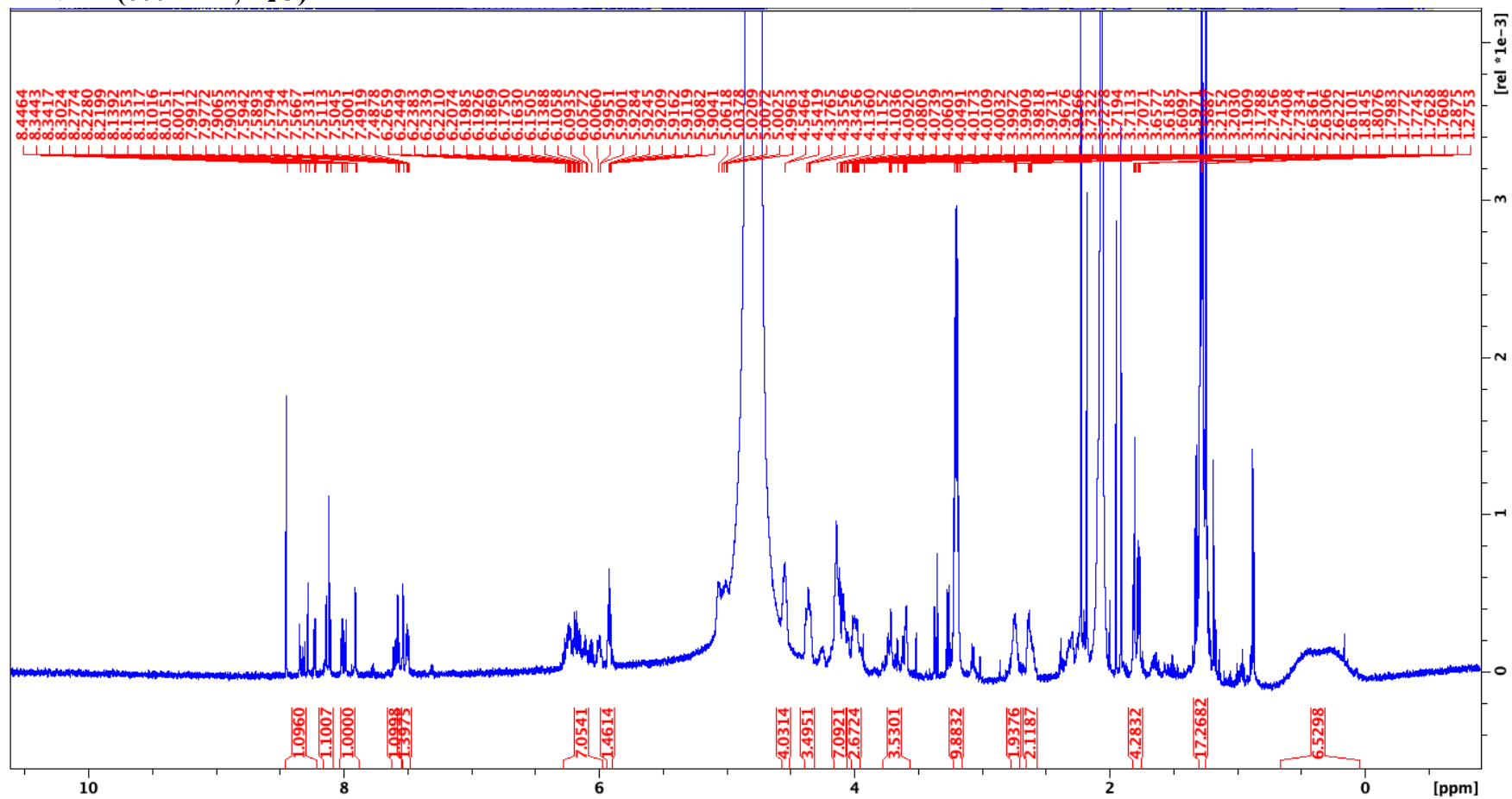


Figure S9 <sup>1</sup>H NMR spectra of PB-DNA tetramer d(C<sub>PB</sub>A<sub>PB</sub>G<sub>PB</sub>T) 16(600 MHz, D<sub>2</sub>O).

**PB/POchimeric tetramer d(C<sub>PB</sub>A<sub>PO</sub>G<sub>PB</sub>T) 17**  
**<sup>1</sup>H NMR (600 MHz, D<sub>2</sub>O)**

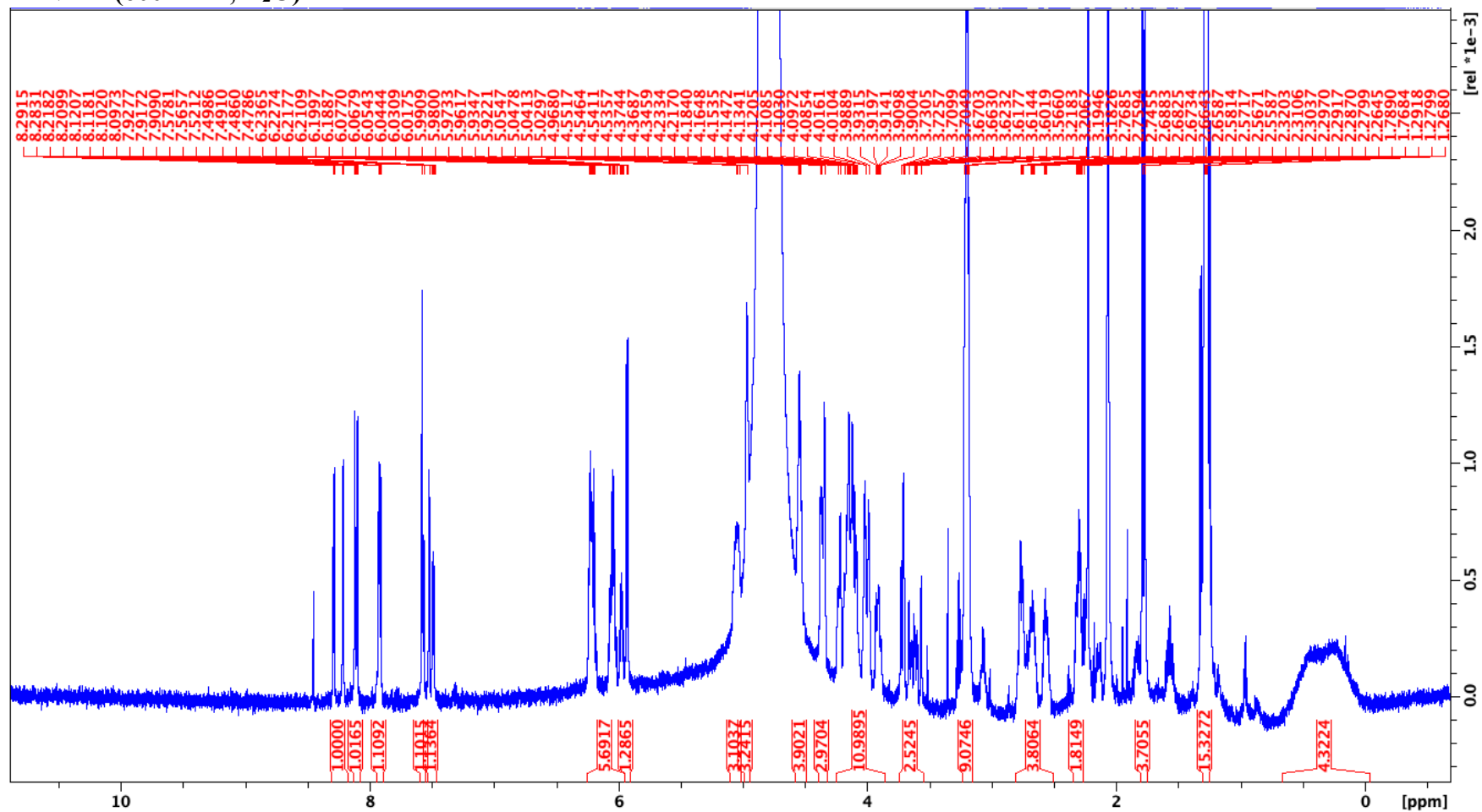


Figure S10 <sup>1</sup>H NMR spectra of PB/POchimeric tetramer d(C<sub>PB</sub>A<sub>PO</sub>G<sub>PB</sub>T) 17 (600 MHz, D<sub>2</sub>O).